Supporting Information for:

De novo designed bifunctional proteins for targeted protein degradation

Bram Mylemans[1,2], Boguslawa Korona[3], Amanda M. Acevedo-Jake[4], Ailsa MacRae[4], Thomas A. Edwards[5], Danny T. Huang[6,7], Andrew J. Wilson[4,8,9]*, Laura S. Itzhaki[3]* and Derek N. Woolfson[1,2,10,11]*

[1]School of Chemistry, University of Bristol, Cantock's Close, Bristol BS8 1TS, UK

[2]Novo Nordisk Foundation Center for Protein Design, Department of Biology and Department of Drug Design and Pharmacology, University of Copenhagen, Jagtvej 160, 2100 Copenhagen, DK

[3]Department of Pharmacology, University of Cambridge, Cambridge CB2 1PD, UK

[4]School of Chemistry, University of Birmingham, Edgbaston, B15 2TT, UK

[5]College of Biomedical Sciences, Larkin University, 18301 N Miami Ave #1, Miami, Florida, 33169 USA

[6]Cancer Research UK Scotland Institute, Garscube Estate, Switchback Road, Glasgow G61 1BD, UK

[7]School of Cancer Sciences, University of Glasgow, Garscube Estate, Switchback Road, Glasgow G61 1QH, UK

[8]School of Chemistry, University of Leeds, Woodhouse Lane, Leeds LS2 9JT, UK

[9]Astbury Centre for Structural Molecular Biology, University of Leeds, Woodhouse Lane, Leeds LS2 9JT, UK

[10]School of Biochemistry, University of Bristol, Medical Sciences Building, University Walk, Bristol BS8 1TD, UK

[11]Max Planck-Bristol Centre for Minimal Biology, University of Bristol, Cantock's Close, Bristol BS8 1TS, UK

*To whom correspondence should be addressed:
a.j.wilson.1@bham.ac.uk; Lsi10@cam.ac.uk; and d.n.woolfson@bristol.ac.uk

Supplementary Table 1. Sequences of peptides used in this study

Name	Sequences	Mass (g/mol)
Sc-apCC-2	Ac–RDRSRLARRRAALKQRIAALKQRRAALKWQIQ SDPRKK QLEQELAALDQEIAAAEQELAALDWQIAG–NH_2	7758.90
BID	Ac–EDIIRNIARHLAQVGDS[Nle]DRSIW–NH_2	2719.03
FAM-BID	FAM–[Ahx]EDIIRNIARHLAQVGDS[Nle]DRSIW–NH_2	3148.47
DAPK1	Ac–LGLPDLVAK–NH_2	966.17
FAM-DAPK1	FAM–[Ahx]LGLPDLVAK–NH_2	1395.60

Supplementary Table 2. Sequences of target protein

Name	Sequences
MCL-1 (172-327)	MGSSHHHHHHSSGLVPRGSHMSDSEVNQEAKPEVKPEVKPETHINLKVSDGSSEIFFKIKKTTPLR RLMEAFAKRQGKEMDSLRFLYDGIRIQADQTPEDLDMEDNDIIEAHREQIGG/ SELYRQSLEIISRYLREQATGAKDTKPMGRSGATSRKALETLRRVGDGVQRNHETAFQGMLRKLDI KNEDDVKSLSRVMIHVFSDGVTNWGRIVTLISFGAFVAKHLKTINQESCIEPLAESITDVLVRTKR DWLVKQRGWDGFVEFFHVEDLEGG
BCL-x$_L$ (1-26 + 81-198	MGSSHHHHHHSSGLVPRGSHMSDSEVNQEAKPEVKPEVKPETHINLKVSDGSSEIFFKIKKTTPLR RLMEAFAKRQGKEMDSLRFLYDGIRIQADQTPEDLDMEDNDIIEAHREQIGG/ MSQSNRELVVDFLSYKLSQKGYSWSQMAAVKQALREAGDEFELRYRRAFSDLTSQLHITPGTAYQS FEQVVNELFRDGVNWGRIVAFFSFGGALCVESVDKEMQVLVSRIAAWMATYLNDHLEPWIQENGGW DTFVELYGNNAAAESRKGQER
KLHL20 (303-605)	MHHHHHHSSGVDLGTENLYFQ/ SMQGPRTRPRKPIRCGEVLFAVGGWCSGDAISSVERYDPQTNEWRMVASMSKRRCGVGVSVLDDLL YAVGGHDGSSYLNSVERYDPKTNQWSSDVAPTSTCRTSVGVAVLGGFLYAVGGQDGVSCLNIVERY DPKENKWTRVASMSTRRLGVAVAVLGGFLYAVGGSDGTSPLNTVERYNPQENRWHTIAPMGTRRKH LGCAVYQDMIYAVGGRDDTTELSSAERYNPRTNQWSPVVAMTSRRSGVGLAVVNGQLMAVGGFDGT TYLKTIEVFDPDANTWRLYGGMNYRRLGGGVGVIKMTHCE

Supplementary Table 3. Sequences of protein binders against MCL-1. MCL-1 binding sites are coloured red

Name	Method	Sequences
Sc-apCC-2-MCL-1-1	Strategy 1	MGSSHHHHHHSSGENLYFQ/ SHMGARLAQLKQERAALEQRLAALDQEIAALEWQIQ SDPRKK QLEQKLLELQAERLRLIGDIVNLDQQILNLEAG
Sc-apCC-2-MCL-1-2	Strategy 1	MGSSHHHHHHSSGENLYFQ/ SHMGAKLLQLKDERLRLIGDLVNLDQEILNLEQQIQ SDPRKK QLEQRLAALKQERAALEQRIAALDWEIAALEAG
Sc-apCC-2-MCL-1-3	Strategy 2 (pAE)	MGSSHHHHHHSSGENLYFQ/ SHMGARLAQLKWERAALKQRLAALDQEIAALTQKIE SDPRKK ELIPRLLRLIGDRVDLERRIAALDQEIAALEAG
Sc-apCC-2-MCL-1-4	Strategy 2 (pLDDT)	MGSSHHHHHHSSGENLYFQ/ SHMGARLEELIAERLRLVGDLVDLDREIAALEQQIQ SDPRKK QLEQRLAALKQERAALEQRIAALDWEIADLDDG
Sc-apCC-2-MCL-1-5	Strategy 2 Selective (Rank pLDDT)	MGSSHHHHHHSSGENLYFQ/ SHMGARLEELITERLRLVGDLLTLDREIAALEQQIQ SDPRKK QLEQRLAALKQERAALEQRIAALDWEIEALEAG
Sc-apCC-2-MCL-1-6	Strategy 2 Selective (Rank combined)	MGSSHHHHHHSSGENLYFQ/ SHMGARLAQLKQERAALKQRLAALDQEIEELEWQIQ SDPRKK QLEQRLLDLIAERLRLVGDIVTLDREIAALEAG

Supplementary Table 4. Sequences of protein binders against BCL-x$_L$. BCL-x$_L$ binding sites are coloured blue

Name	**Method**	**Sequences**
Sc-apCC-2-BCL-x$_L$-1	Strategy 1 (pAE)	MGSSHHHHHHSSGENLYFQ/ SHMGARLAQLKQERAALKQRLAALDQEIAALEWQIQ SDPRKK QLYQRLLALISDRFALEQRIAALDQEIAALEAG
Sc-apCC-2-BCL-x$_L$-2	Strategy 1 (pLDDT)	MGSSHHHHHHSSGENLYFQ/ SHMGARLAQLKQERAALKQRLAALDQEIAALEWQIQ SDPRKK QLIQRLLALISDRFALEQRIAALDQEIAALEAG
Sc-apCC-2-BCL-x$_L$-3	Strategy 2 (pAE)	MGSSHHHHHHSSGENLYFQ/ SHMGARLAQLKQERAALKQRLEALDQEIAALEWQIQ SDPRKK QLQQRLRELIGERLRLFGDIFQLDVEIAALEAG
Sc-apCC-2-BCL-x$_L$-4	Strategy 2 (pAE)	MGSSHHHHHHSSGENLYFQ/ SHMGARLAQLKQERAALKQRLDALDQEIAALEWQIQ SDPRKK QLYQRLVELIGERLRLISDIFELDVEIAALEAG
Sc-apCC-2-BCL-x$_L$-5	Strategy 2 (pLDDT)	MGSSHHHHHHSSGENLYFQ/ SHMGARLAQLKQERAALKQRLDALDQEIAALEWQIQ SDPRKK QLYQRLLELIGERLALMGDIFELDVEIAALEAG
Sc-apCC-2-BCL-x$_L$-6	Strategy 2 (pLDDT)	MGSSHHHHHHSSGENLYFQ/ SHMGARLAQLKQERAALKQRLEALDQEIAALEWQIQ SDPRKK QLIQRLRELFGERLSLMGDIFQLDVEIAALEAG
Sc-apCC-2-BCL-x$_L$-7	Strategy 2 (ΔG)	MGSSHHHHHHSSGENLYFQ/ SHMGARLAQLKQERAALKQRLAALDQEIEALEWQIQ SDPRKK QLFGRLLSLFGDRFDLERRIAALDQEIAALEAG
Sc-apCC-2-BCL-x$_L$-8	Strategy 2 (ΔG)	MGSSHHHHHHSSGENLYFQ/ SHMGARLAQLKQERAALKQRLEALDQEIAALEWQIQ SDPRKK QLLQRLYELFGERLALFGDIFDLDVEIAALEAG
Sc-apCC-2-BCL-x$_L$-9	Strategy 2 (Sc)	MGSSHHHHHHSSGENLYFQ/ SHMGARLAQLKQERAALKQRLAALDQEIAALEWQIQ SDPRKK QLFGRLLGLMGDRFELEQRIAALDQEIAALEAG
Sc-apCC-2-BCL-x$_L$-10	Strategy 2 (Sc)	MGSSHHHHHHSSGENLYFQ/ SHMGARLAQLKQERAALKQRLAALDQEIEALEWQIQ SDPRKK QLFGRLLSLFSDRFDLERRIAALDQEIAALEAG
Sc-apCC-2-BCL-x$_L$-11	Strategy 3 (pAE)	MGSSHHHHHHSSGENLYFQ/ SHMGPELAALQAERDALEARLAELDREIAALEWRIP SDPRKK QLIGELLRLFGDRFDLERRIAELDAKIEALKNG
Sc-apCC-2-BCL-x$_L$-12	Strategy 3 (pLDDT)	MGSSHHHHHHSSGENLYFQ/ SHMGPELERLEERRRELERELEELDREIAELEWTIK SDPRKK ELIVKLRQLFGRRLRLMGDIFDLDVQIRRLREG
Sc-apCC-2-BCL-x$_L$-13	Strategy 4 (pAE)	MGSSHHHHHHSSGENLYFQ/ SHMGARLAQLKQERAALKQRLAALDQEIAALEWQIQ SDPRKV QLWGRLLGLLADRFELEQRIAALDQEIAALEAG
Sc-apCC-2-BCL-x$_L$-14	Strategy 4 (pLDDT)	MGSSHHHHHHSSGENLYFQ/ SHMGARLAQLKQERAALKQRLDALEQEIAALEWQIQ SDPRKK QLQQRLRQLYGERLRLESDIFDLDVEIAALEAG
Sc-apCC-2-BCL-x$_L$-15	Strategy 2 Selective (rank pLDDT)	MGSSHHHHHHSSGENLYFQ/ SHMGARLAQLKQERAALKQRLEALDQEIAALEWQIQ SDPRKK QLQQRLRELIGERLRLMGDIFQLDVEIAALEAG
Sc-apCC-2-BCL-x$_L$-16	Strategy 2 Selective (rank pAE)	MGSSHHHHHHSSGENLYFQ/ SHMGARLAQLKQERAALKQRLDALDQEIAALEWQIQ SDPRKK QLLQRLRELIGERLRLISDIFDLDVEIAALEAG
Sc-apCC-2-BCL-x$_L$-17	Strategy 2 Selective (rank Sc)	MGSSHHHHHHSSGENLYFQ/ SHMGARLAQLKQERAALKQRLAALDQEIAALEWQIQ SDPRKK QLLERLRRLFGERLRLFSDIFQLDQEIAALEAG
Sc-apCC-2-BCL-x$_L$-18	Strategy 2 Selective (rank combined)	MGSSHHHHHHSSGENLYFQ/ SHMGARLAQLKQERAALKQRLEALDQEIAALEWQIQ SDPRKK QLLQRLRRLYGERLALFGDIFDLDVEIAALEAG

Supplementary Table 6. Sequences of protein binders against KLHL20. KLHL20 binding sites are coloured yellow

Name	Method	Sequences
Sc-apCC-2-KLHL20-1	Short loop natural	MGSSHHHHHHSSGENLYFQ/ SHMGARLAQLKQERAALKQRLAALDQEIAALEWQIQA GLPDLVG AQLEQRLAALKQERAALEQRIAALDQEIAALEAG
Sc-apCC-2-KLHL20-2	Long loop natural	MGSSHHHHHHSSGENLYFQ/ SHMGARLAQLKQERAALKQRLAALDQEIAALEWQIQA GLGLPDLVAKYNG AQLEQRLAALKQERAALEQRIAALDQEIAALEAG
Sc-apCC-2-KLHL20-3	Short loop MPNN	MGSSHHHHHHSSGENLYFQ/ SHMGARLAQLKQERAALKQRLAALDQEIAALQARIDA GAPDLVR PVLEARLAALKQERAALEQRIAALDWEIAALEAG
Sc-apCC-2-KLHL20-4	Long loop MPNN	MGSSHHHHHHSSGENLYFQ/ SHMGARLAQLKQERAALKQRLAALDQEIAALEWQIQ QAKTLPDLVREVV VSQLEQRLAALKQERAALEQRIAALDQEIAALEAG

Supplementary Table 7. Sequences of bifunctional protein binders. BCL-x$_L$ binding sites are coloured blue, KLHL20 binding sites are coloured yellow

Name	Sequences
Sc-apCC-2-BCL-x$_L$-5 - KLHL20-3	MGSSHHHHHHSSGENLYFQ/ SHMGARLAQLKWERAALKQRLAALDQEIAALQARIDA GAPDLVR PVLYQRLLELIGERLALMGDIFELDVEIAALEAG

Supplementary Table 8. Sequences of constructs used in GFP-assay see Figure 12. Linkers between domains in lower case, MCL-1 binding sites are coloured red. BCL-x$_L$ binding sites are coloured blue, KLHL20 binding sites are coloured yellow

Construct	Sequence
Construct for stable cell line generation	
eGFP-BCL-x$_L$ 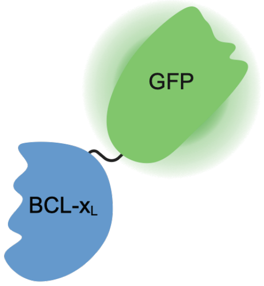 	MVSKGEELFTGVVPILVELDGDVNGHKFSVSGEGEGDATYGKLTLKFICT TGKLPVPWPTLVTTLTYGVQCFSRYPDHMKQHDFFKSAMPEGYVQERTIF FKDDGNYKTRAEVKFEGDTLVNRIELKGIDFKEDGNILGHKLEYNYNSHN VYIMADKQKNGIKVNFKIRHNIEDGSVQLADHYQQNTPIGDGPVLLPDNH YLSTQSALSKDPNEKRDHMVLLEFVTAAGITLGMDELYKVDPVAGA ggsggggs MSQSNRELVVDFLSYKLSQKGYSWSQFSDVEENRTEAPEGTESEMETPSA INGNPSWHLADSPAVNGATAHSSSLDAREVIPMAAVKQALREAGDEFELR YRRAFSDLTSQLHITPGTAYQSFEQVVNELFRDGVNWGRIVAFFSFGGAL CVESVDKEMQVLVSRIAAWMATYLNDHLEPWIQENGGWDTFVELYGNNAA AESRKGQERFNRWFLTGMTVAGVVLLGSLFSRK
Full construct for BCL-x$_L$ assay	
3xHA-[Targeting-domain]-SPOP(167-374)-T2A-mCherry 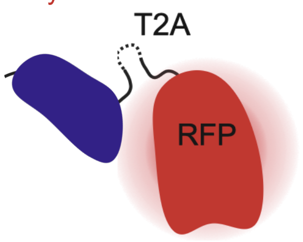 	YPYDVPDYAYPYDVPDYAYPYDVPDYAgsdq [Targeting-domain] gssgsg SVNISGQNTMNMVKVPECRLADELGGLWENSRFTDCCLCVAGQEFQAHKA ILAARSPVFSAMFEHEMEESKKNRVEINDVEPEVFKEMMCFIYTGKAPNL DKMADDLLAAADKYALERLKVMCEDALCSNLSVENAAEILILADLHSADQ LKTQAVDFINYHASDVLETSGWKSMVVSHPHLVAEAYRSLASAQCPFLGP PRKRLKQS gssggsgEGRGSLLTCGDVEENPG/Pggsg VSKGEEDNMAIIKEFMRFKVHMEGSVNGHEFEIEGEGEGRPYEGTQTAKL KVTKGGPLPFAWDILSPQFMYGSKAYVKHPADIPDYLKLSFPEGFKWERV MNFEDGGVVTVTQDSSLQDGEFIYKVKLRGTNFPSDGPVMQKKTMGWEAS SERMYPEDGALKGEIKQRLKLKDGGHYDAEVKTTYKAKKPVQLPGAYNVN IKLDITSHNEDYTIVEQYERAEGRHSTGGMDELYK
Targeting domain	
Sc-apCC-2-MCL-1-1	…

	GARLAQLKQERAALEQRLAALDQEIAALEWQIQ SDPRKK QLEQKLLELQAERLRLIGDIVNLDQQILNLEAG …
αGFP	… VQLVESGGALVQPGGSLRLSCAASGFPVNRYSMRWYRQAPGKEREWVAGM SSAGDRSSYEDSVKGRFTISRDDARNTVYLQMNSLKPEDTAVYYCNVNVG FEYWGQGTQVTVSS …
Sc-apCC-2-BCL-x$_L$-3	… GARLAQLKQERAALKQRLEALDQEIAALEWQIQ SDPRKK QLQQRLRELIGERLRLFGDIFQLDVEIAALEAG …
Sc-apCC-2-BCL-x$_L$-4	… GARLAQLKQERAALKQRLDALDQEIAALEWQIQ SDPRKK QLYQRLVELIGERLRLISDIFELDVEIAALEAG …
Sc-apCC-2-BCL-x$_L$-5	… GARLAQLKQERAALKQRLDALDQEIAALEWQIQ SDPRKK QLYQRLLELIGERLALMGDIFELDVEIAALEAG …
Sc-apCC-2-BCL-x$_L$-6	… GARLAQLKQERAALKQRLEALDQEIAALEWQIQ SDPRKK QLIQRLRELFGERLSLMGDIFQLDVEIAALEAG …
Sc-apCC-2-BCL-x$_L$-7	… GARLAQLKQERAALKQRLAALDQEIEALEWQIQ SDPRKK QLFGRLLSLFGDRFDLERRIAALDQEIAALEAG …
Sc-apCC-2-BCL-x$_L$-8	… GARLAQLKQERAALKQRLEALDQEIAALEWQIQ SDPRKK QLLQRLYELFGERLALFGDIFDLDVEIAALEAG …
Sc-apCC-2-BCL-x$_L$-9	… GARLAQLKQERAALKQRLAALDQEIAALEWQIQ SDPRKK QLFGRLLGLMGDRFELEQRIAALDQEIAALEAG …
Sc-apCC-2-BCL-x$_L$-10	… GARLAQLKQERAALKQRLAALDQEIEALEWQIQ SDPRKK ›QLFGRLLSLFSDRFDLERRIAALDQEIAALEAG …
Full construct for KLHL20 assay	
3xHA-αGFP-[Degron domain]-T2A-mCherry 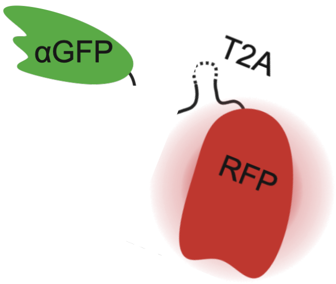 	YPYDVPDYAYPYDVPDYAYPYDVPDYAgsdq VQLVESGGALVQPGGSLRLSCAASGFPVNRYSMRWYRQAPGKEREWVAG MSSAGDRSSYEDSVKGRFTISRDDARNTVYLQMNSLKPEDTAVYYCNVN VGFEYWGQGTQVTVSS [Degron–domain] gssggsgEGRGSLLTCGDVEENPG/Pggsg VSKGEEDNMAIIKEFMRFKVHMEGSVNGHEFEIEGEGEGRPYEGTQTAK LKVTKGGPLPFAWDILSPQFMYGSKAYVKHPADIPDYLKLSFPEGFKWE RVMNFEDGGVVTVTQDSSLQDGEFIYKVKLRGTNFPSDGPVMQKKTMGW EASSERMYPEDGALKGEIKQRLKLKDGGHYDAEVKTTYKAKKPVQLPGA YNVNIKLDITSHNEDYTIVEQYERAEGRHSTGGMDELYK
Degron domain	
KLHL20d	…

	LLAMNLGLPDLVAKYNTSNGAgsgsLLAMNLGLPDLVAKYNTSNGAgsgsLLAMNLGLPDLVAKYNTSNGA …
Sc-apCC-2-KLHL20-1	… GARLAQLKQERAALKQRLAALDQEIAALEWQIQA GLPDLVGAQLEQRLAALKQERAALEQRIAALDQEIAALEAG …
Sc-apCC-2-KLHL20-2	… GARLAQLKQERAALKQRLAALDQEIAALEWQIQA GLGLPDLVAKYNGAQLEQRLAALKQERAALEQRIAALDQEIAALEAG …
Sc-apCC-2-KLHL20-3	… GARLAQLKQERAALKQRLAALDQEIAALQARIDA GAPDLVRPVLEARLAALKQERAALEQRIAALDWEIAALEAG …
Sc-apCC-2-KLHL20-4	… GARLAQLKQERAALKQRLAALDQEIAALEWQIQ QAKTLPDLVREVVVSQLEQRLAALKQERAALEQRIAALDQEIAALEAG …

Supplementary Table 9. Sequences of constructs used in endogenous degradation and apoptosis assay Linkers between domains in lower case, BCL-x$_L$ binding sites are coloured blue, KLHL20 binding sites are coloured yellow

Construct	**Sequence**
Full construct for endogenous degradation	
3xHA-[Degradation domain]-T2A-mCherry 	YPYDVPDYAYPYDVPDYAYPYDVPDYAgsdq [Degradation domain] gssggsgEGRGSLLTCGDVEENPG/PggsgVSKGEEDNMAIIKEFMRFKVHMEGSVNGHEFEIEGEGEGRPYEGTQTAKLKVTKGGPLPFAWDILSPQFMYGSKAYVKHPADIPDYLKLSFPEGFKWERVMNFEDGGVVTVTQDSSLQDGEFIYKVKLRGTNFPSDGPVMQKKTMGWEASSERMYPEDGALKGEIKQRLKLKDGGHYDAEVKTTYKAKKPVQLPGAYNVNIKLDITSHNEDYTIVEQYERAEGRHSTGGMDELYK
Degradation domain	
Sc-apCC-2-BCLx$_L$-5	… GARLAQLKQERAALKQRLDALDQEIAALEWQIQSDPRKKQLYQRLLELIGERLALMGDIFELDVEIAALEAG …
Sc-apCC-2-KLHL20-3	… GARLAQLKQERAALKQRLAALDQEIAALQARIDAGAPDLVRPVLEARLAALKQERAALEQRIAALDWEIAALEAG …
Sc-apCC-2-BCLx$_L$-5-KLHL20-3	… GARLAQLKWERAALKQRLAALDQEIAALQARIDAGAPDLVRPVLYQRLLELIGERLALMGDIFELDVEIAALEAG …
Sc-apCC-2-BCLx$_L$-5_Sc-apCC-2-KLHL20-3	… GARLAQLKQERAALKQRLDALDQEIAALEQQIQSDPRKKQLYQRLLELIGERLALMGDIFELDVEIAALEAGGGSGGSGARLAQLKQERAALKQRLAALDQEIAALQARIDAGAPDLVRPVLEARLAALKQERAALEQRIAALDWEIAALEAG …
Sc-apCC-2-KLHL20-4	…

	GARLAQLKQERAALKQRLAALDQEIAALEWQIQQAKTLPDLVREVVVSQLEQRLAALKQERAALEQRIAALDQEIAALEAG …
Sc-apCC-2-BCLx$_L$-9-KLHL20-4	… GARLAQLKWERAALKQRLAALDQEIAALEQQIQQAKTLPDLVREVVVSQLFGRLLGLMGDRFELEQRIAALDQEIAALEAG …
Sc-apCC-2-BCLx$_L$-9_Sc-apCC-2-KLHL20-3	… GARLAQLKQERAALKQRLAALDQEIAALEQQIQSDPRKKQLFGRLLGLMGDRFELEQRIAALDQEIAALEAGGGSGGSGARLAQLKQERAALKQRLAALDQEIAALQARIDAGAPDLVRPVLEARLAALKQERAALEQRIAALDWEIAALEAG…
Sc-apCC-2-BCLx$_L$-10-KLHL20-4	… GARLAQLKQERAALKQRLAALDQEIAALEQQIQQAKTLPDLVREVVVSQLFGRLLSLFSDRFDLERRIAALDQEIAALEAG …
Sc-apCC-2-BCLx$_L$-10_Sc-apCC-2-KLHL20-3	… GARLAQLKQERAALKQRLAALDQEIEALEQQIQSDPRKKQLFGRLLSLFSDRFDLERRIAALDQEIAALEAGGGSGGSGARLAQLKQERAALKQRLAALDQEIAALQARIDAGAPDLVRPVLEARLAALKQERAALEQRIAALDWEIAALEAG …

Supplementary Table 10. Sequence motifs used in BCL-2 family designs

Name	Motif Sequences			
BCL-x$_L$	Y...L..IGD.F	I...L..IGD.F	F...L..IGD.F	
	Y...L..FGD.F	I...L..FGD.F	F...L..FGD.F	
	Y...L..ISD.F	I...L..ISD.F (BIM)	F...L..ISD.F	
	Y...L..FSD.F	I...L..FSD.F	F...L..FSD.F	
	Y...L..MSD.F (BAD)	I...L..MSD.F	F...L..MSD.F	
	Y...L..MGD.F	I...L..MGD.F	F...L..MGD.F	
MCL-1	I...L..IGD.F	I...L..IGD.L	I...L..IGD.V (NOXA-B)	I...L..IGD.M
	I...L..VGD.F	I...L..VGD.L	I...L..VGD.V	I...L..VGD.M
	I...L..IAD.F	I...L..IAD.L	I...L..IAD.V	I...L..IAD.M
	I...L..VAD.F	I...L..VAD.L	I...L..VAD.V	I...L..VAD.M

Supplementary Table 11. Measured K$_D$'s of used tracers in competition assays

Name	Target	K$_D$ (nM)
BID-FAM	MCL-1	21.5 ± 1.1
BID-FAM	BCL-x$_L$	71 ± 8.4
DAPK1-FAM	KLHL20	12 200 ± 800

Supplementary Table 12. Measured IC$_{50}$ values against the BCL-2 family targets

Name design	**IC_{50} BCL-x_L (nM)**	**IC_{50} MCL-1 (nM)**
Sc-apCC-2-MCL-1-1	Non-binding	230 ± 20
Sc-apCC-2-MCL-1-2	Non-binding	13 000 ± 2 000
Sc-apCC-2-MCL-1-3	40 000 ± 20 000	64 ± 2
Sc-apCC-2-MCL-1-4	20 000 ± 5 000	230 ± 30
Sc-apCC-2-MCL-1-5	100 000 ± 16 000	810 ± 70
Sc-apCC-2-MCL-1-6	100 000 ± 20 000	1 020 ± 90
Sc-apCC-2-BCL-x_L-1	Non-binding.	Non-binding
Sc-apCC-2-BCL-x_L-2	Non-binding	Non-binding
Sc-apCC-2-BCL-x_L-3	196 ± 14	660 ± 50
Sc-apCC-2-BCL-x_L-4	4 600 ± 600	18 000 ± 3 000
Sc-apCC-2-BCL-x_L-5	230 ± 20	68 ± 4
Sc-apCC-2-BCL-x_L-6	198 ± 130	640 ± 60
Sc-apCC-2-BCL-x_L-7	260 ± 20	1 150 ± 90
Sc-apCC-2-BCL-x_L-8	250 ± 7	193 ± 12
Sc-apCC-2-BCL-x_L-9	300 ± 30	3 080 ± 180
Sc-apCC-2-BCL-x_L-10	430 ± 30	26 000 ± 8 000
Sc-apCC-2-BCL-x_L-11	197 ± 10	500 ± 150
Sc-apCC-2-BCL-x_L-12	212 ± 18	270 ± 20
Sc-apCC-2-BCL-x_L-13	1 390 ± 40	9 200± 70
Sc-apCC-2-BCL-x_L-15	109 ± 14	218 ± 11
Sc-apCC-2-BCL-x_L-16	3 000 ± 400	90 000± 70 000
Sc-apCC-2-BCL-x_L-17	52 ± 3	68 000± 80 000
Sc-apCC-2-BCL-x_L-5-KLHL20-3	45 ± 2	Not applicable

Supplementary Table 13. Measured IC_{50} values against KLHL20

Name design	**IC_{50} KLHL20 (µM)**
Sc-apCC-2-KLHL20-1	3.9 ± 0.2
Sc-apCC-2-KLHL20-2	2.18 ± 0.16
Sc-apCC-2-KLHL20-3	3.16 ± 0.18
Sc-apCC-2-KLHL20-4	1.35 ± 0.17
Sc-apCC-2-BCL-x_L-5-KLHL20-3	2.5 ± 0.2

Supplementary Table 14. ITC fitting and thermodynamic annalysis

	Sc-apCC-2-BCL-x_L-3
Number of binding sites	0.86
K_D	3 nM
ΔG	-12 kcal/mol
ΔH	-2.3 kcal/mol
$T\Delta S$	9.7 kcal/mol

Supplementary Table 15. Crystallisation conditions

Crystal structure	**Crystal screen**	**Composition**
Sc-apCC-2	JCSG+ A6	0.2 M Lithium sulphate, 0.1 M Phosphate/ citrate pH 4.2 20% w/v PEG1000
Sc-apCC-2-MCL-1-1	JCSG+ D4	0.2 M Lithium sulphate, 0.1 M Sodium acetate pH 4.5, 30% w/v PEG8000
Sc-apCC-2-BCL-x$_L$-2	Morpheus G9	0.02 M Sodium formate, 0.02 M Ammonium, acetate; 0.2M Sodium citrate tribasic, Dihydrate, 0.02 M Potassium sodium tartrate tetrahydrate, 0.02 M Sodium oxamate, 0.01 M Tris, 0.01M BICINE pH 8.5, 20% v/v PEG 500 MME; 10% w/v PEG 20000
Sc-apCC-2-BCL-x$_L$-5	Proplex G12	1.0 M Sodium citrate tribasic dihydrate, 0.1 M Sodium HEPES pH 7.0
Sc-apCC-2-BCL-x$_L$-6	Morpheus C5	0.03 M Sodium nitrate, 0.03 M Sodium phosphate dibasic, 0.03 M Ammonium sulphate, 0.01 M HEPES, 0.01 MOPS pH 7.5, 20% v/v PEG 500 MME; 10% w/v PEG 20000
Sc-apCC-2-BCL-x$_L$-8	Proplex B6	0.1 M Sodium HEPES pH 7.0, 10 % w/v PEG4000, 10 % v/v 2-Propanol
Sc-apCC-2-BCL-x$_L$-11	JCSG+ F10	1.1 M Sodium malonate dibasic monohydrate, 0.1 M HEPES pH 7.0, 0.5 % v/v Jeffamine® ED-2003
Sc-apCC-2-BCL-x$_L$-3: BCL-x$_L$	MPD E1	0.1 M Citric acid pH 4.0, 10% v/v MPD
Sc-apCC-2-MCL-1-3:MCL-1	Morpheus A12	0.03 M Magnesium chloride hexahydrate, 0.03 M Calcium chloride dihydrate, 0.01 M Tris, 0.01M BICINE pH 8.5, 2.5% v/v MPD; 12.5% PEG1000; 12.5% w/v PEG3350
Sc-apCC-2-MCL-1-4:MCL-1	JCSG+ B4	0.1 M HEPES pH7.5, 10% w/v PEG8000, 8% v/v ethylene glycol
Sc-apCC-2-KLHL20-3	Proplex D2	0.1 M MES pH 6.5, 10% w/v PEG5000MME, 12% v/v 1-Propanol
Sc-apCC-2-KLHL20-4	Proplex B12	0.1 M Magnesium chloride hexahydrate, 0.1 M Sodium HEPES pH 7.0, 15 % w/v PEG4000

Supplementary Table 16. Merging and refinement statistics for all X-ray structures

	Sc-apCC-2	**Sc-apCC-2-MCL-1-1**	**Sc-apCC-2-BCL-xL-2**	**Sc-apCC-2-BCL-xL-5**	**Sc-apCC-2-BCL-xL-6**
PDB code	9TLL	9TLM	9TLN	9TLO	9TLP
Resolution range	34.11 - 1.5 (1.55 - 1.5)	30.99 - 1.8 (1.86 - 1.8)	32.36 - 1.15 (1.19 - 1.15)	45.09 - 2.2 (2.28 - 2.2)	33.48 - 1.75 (1.81 - 1.75)
Space group	I 41	P 65 2 2	P 41 2 2	P 43 21 2	P 1
Unit cell	48.237 48.237 70.272 90 90 90	71.578 71.578 90.456 90 90 120	37.573 37.573 127.365 90 90 90	69.57 69.57 112.756 90 90 90	29.211 46.11 54.103 90.51 96.519 106.022
Total reflections	180234 (10441)	516546 (51414)	921551 (55532)	386222 (38535)	95560 (8302)
Unique reflections	15585 (1430)	13253 (1274)	38224 (3760)	14682 (1417)	26841 (2646)
Multiplicity	11.6 (7.3)	39.0 (40.4)	24.1 (14.8)	26.3 (27.2)	3.6 (3.1)
Completeness (%)	99.44 (97.25)	99.91 (99.69)	99.85 (99.76)	99.95 (100.00)	98.78 (96.99)
Mean I/sigma(I)	11.04 (1.81)	25.97 (1.62)	16.70 (0.78)	13.06 (2.22)	20.24 (10.87)
Wilson B-factor	13.69	35.73	16.23	37.54	14.62
R-pim	0.06743 (0.845)	0.0142 (0.5129)	0.01382 (0.8239)	0.03813 (0.3654)	0.02126 (0.04552)
CC1/2	0.955 (0.109)	1 (0.789)	1 (0.653)	0.999 (0.764)	0.999 (0.991)
Reflections used in refinement	12808 (1240)	13235 (1269)	33510 (3261)	14674 (1417)	26834 (2646)
Reflections used for R-free	617 (63)	643 (63)	1645 (162)	765 (71)	1337 (123)
R-work	0.1808 (0.1978)	0.2460 (0.3640)	0.1880 (0.2835)	0.2112 (0.2480)	0.1542 (0.1865)
R-free	0.1955 (0.2246)	0.2599 (0.3316)	0.2054 (0.3381)	0.2468 (0.2737)	0.2012 (0.2501)
Ramachandran favored (%)	100	100	100	98.57	99.3
Ramachandran allowed (%)	0	0	0	0.95	0.7
Ramachandran outliers (%)	0	0	0	0.48	0
Rotamer outliers (%)	0	1.67	1.72	0	0.43
Clashscore	3.45	0.83	2.45	1.76	3.15
Average B-factor	19.44	39.74	24.47	49.74	17.92

Supplementary Table 16 cont. Merging and refinement statistics for all X-ray structures

	Sc-apCC-2-BCL-xL-8	**Sc-apCC-2-BCL-xL-11**	**Sc-apCC-2-KLHL20-3**	**Sc-apCC-2-KLHL20-4**
PDB code	9TLQ	9TLR	9TLS	9TLT
Resolution range	49.15 - 2.6 (2.69 - 2.6)	29.4 - 1.95 (2.02 - 1.95)	29.37 - 1.45 (1.5 - 1.45)	36.74 - 1.95 (2.02 - 1.95)
Space group	P 32 2 1	I 41 2 2	P 1 21 1	P 1
Unit cell	113.501 113.501 86.29 90 90 120	58.696 58.696 83.329 90 90 90	49.903 31.91 75.183 90 93.523 90	47.834 53.711 73.656 74.218 72.058 65.315
Total reflections	410191 (41958)	128744 (7468)	286321 (23648)	90871 (9034)
Unique reflections	20112 (2010)	5598 (556)	42389 (4145)	45552 (4529)
Multiplicity	20.4 (20.9)	23.0 (13.4)	6.8 (5.7)	2.0 (2.0)
Completeness (%)	99.87 (99.80)	99.96 (100.00)	99.88 (98.97)	99.90 (100.00)
Mean I/sigma(I)	15.49 (2.05)	15.67 (2.25)	12.22 (1.95)	18.28 (7.22)
Wilson B-factor	62.89	31.36	18.34	16.16
R-pim	0.02497 (0.2766)	0.02474 (0.3094)	0.02967 (0.3854)	0.02586 (0.06315)
CC1/2	0.999 (0.903)	0.999 (0.809)	0.999 (0.835)	0.998 (0.986)
Reflections used in refinement	20086 (2006)	5596 (556)	42379 (4143)	45499 (4528)
Reflections used for R-free	939 (81)	281 (25)	2124 (214)	2197 (221)
R-work	0.2439 (0.3053)	0.2207 (0.2623)	0.1804 (0.2437)	0.1755 (0.1909)
R-free	0.2758 (0.3861)	0.2455 (0.2930)	0.2104 (0.2946)	0.2226 (0.2584)
Ramachandran favored (%)	96.68	95.71	99.55	98.59
Ramachandran allowed (%)	3.32	4.29	0.45	1.41
Ramachandran outliers (%)	0	0	0	0
Rotamer outliers (%)	0.64	0	0	0.8
Clashscore	2.97	2.76	3.77	2.27
Average B-factor	81.3	38.31	25.85	18.45

Supplementary Table 16 cont. Merging and refinement statistics for all X-ray structures

	BCL-xL:Sc-apCC-2-BCL-xL-3	MCL-1:Sc-apCC-2-MCL-1-3	MCL-1:Sc-apCC-2-MCL-1-4
PDB code	9TLU	9TLV	9TLW
Resolution range	73.99 - 2.99 (3.42 - 2.99)	57.52 - 2.0 (2.07 - 2.0)	58.34 - 2.8 (2.9 - 2.8)
Space group	P 61	P 1 21 1	P 1 21 1
Unit cell	85.441 85.441 145.517 90 90 120	62.194 57.952 63.079 90 114.239 90	50.353 83.881 63.379 90 113.005 90
Total reflections	410169 (54651)	379065 (35888)	141612 (13278)
Unique reflections	20106 (2546)	27768 (2749)	20306 (2024)
Multiplicity	20.4 (21.5)	13.7 (13.1)	7.0 (6.6)
Completeness (%)	99.91 (99.95)	99.31 (98.06)	99.79 (99.70)
Mean I/sigma(I)	15.49 (5.23)	18.90 (9.42)	10.62 (3.44)
Wilson B-factor	77.44	23.14	44.68
R-pim	0.02495 (0.1131)	0.02171 (0.08759)	0.03238 (0.1764)
CC1/2	0.999 (0.975)	0.999 (0.961)	0.997 (0.963)
Reflections used in refinement	12190 (4059)	27658 (2729)	12024 (1196)
Reflections used for R-free	544 (184)	1323 (138)	572 (53)
R-work	0.2747 (0.3626)	0.2081 (0.2362)	0.2483 (0.2988)
R-free	0.3216 (0.4027)	0.2559 (0.2718)	0.2948 (0.3665)
Ramachandran favored (%)	94.12	98.13	98.68
Ramachandran allowed (%)	5.39	1.87	1.32
Ramachandran outliers (%)	0.49	0	0
Rotamer outliers (%)	0.93	0.31	2.23
Clashscore	13.38	4.44	9.47
Average B-factor	79.19	30.62	60.82

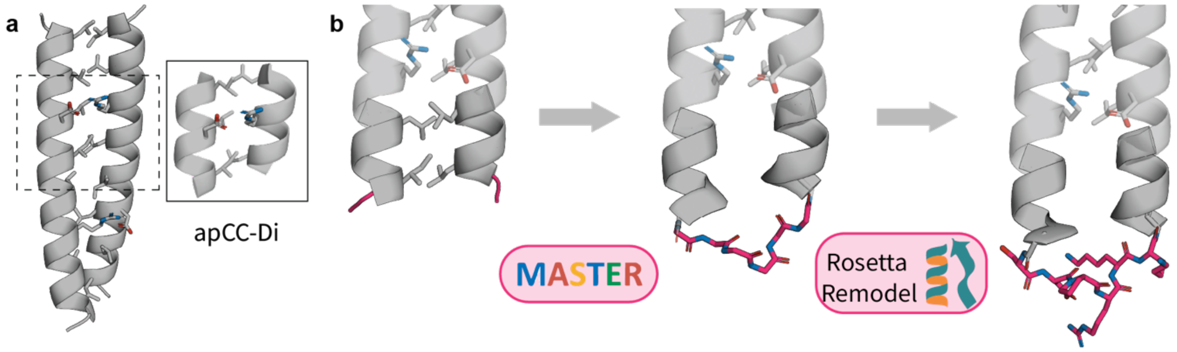

Supplementary Figure 1. Schematic of loop design a, Structure of the apCC-Di (PDB: 7Q1R) peptide. The zoom-in shows the key aspartate-arginine pair. **b,** Schematic of the loop design. First, the final 7 residues of each helix are used as MASTER search motif. MASTER was used to identify different gap length in between the two helices, ranging from 3 to 6. As 4 residue loops were the most common, the top hit was used. The sequence of this loop was subsequently redesigned with Rosetta Remodel.

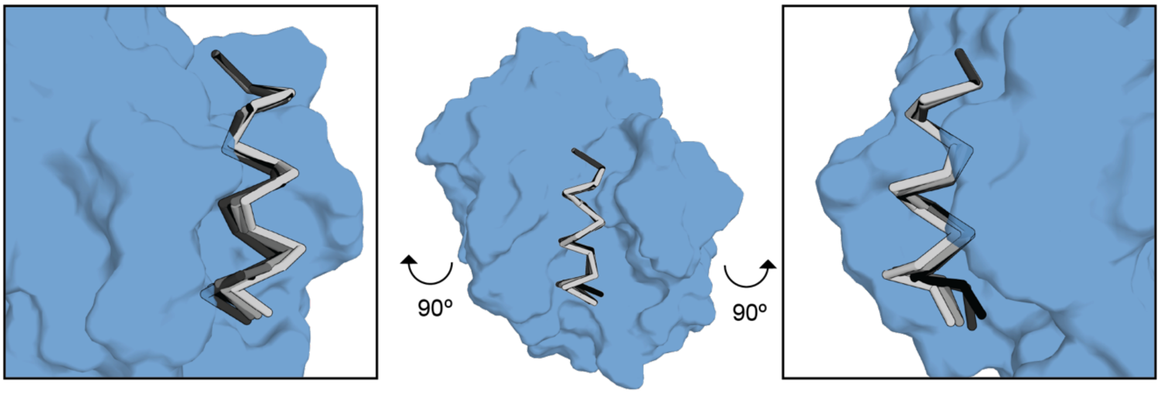

Supplementary Figure 2. Different models for binder alignment. Models of BCL-x_L (blue) in complex with a peptide effector. The position of the effector (black to light grey) was varied slightly with a Rosetta script to generate different starting poses

Sc-apCC-2-MCL-1-1

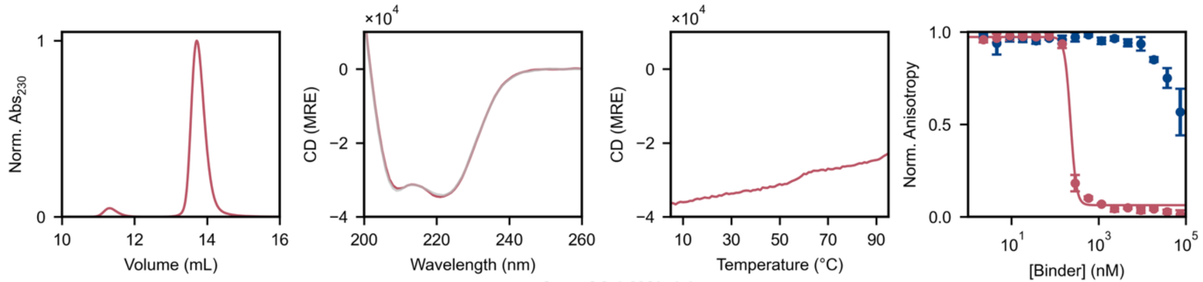

Sc-apCC-2-MCL-1-2

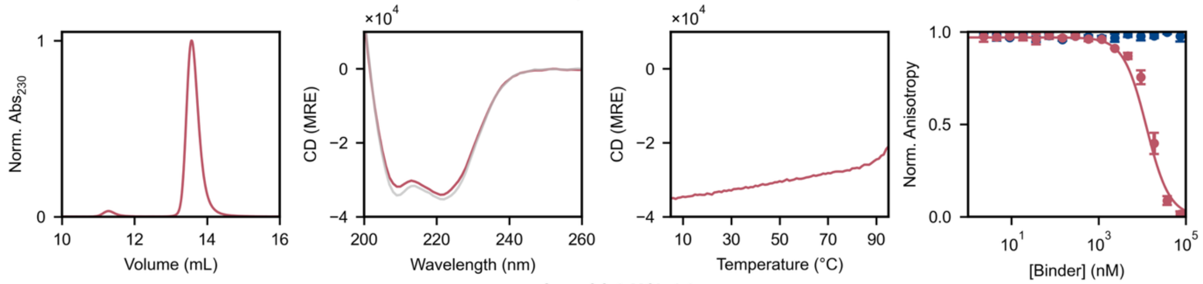

Sc-apCC-2-MCL-1-3

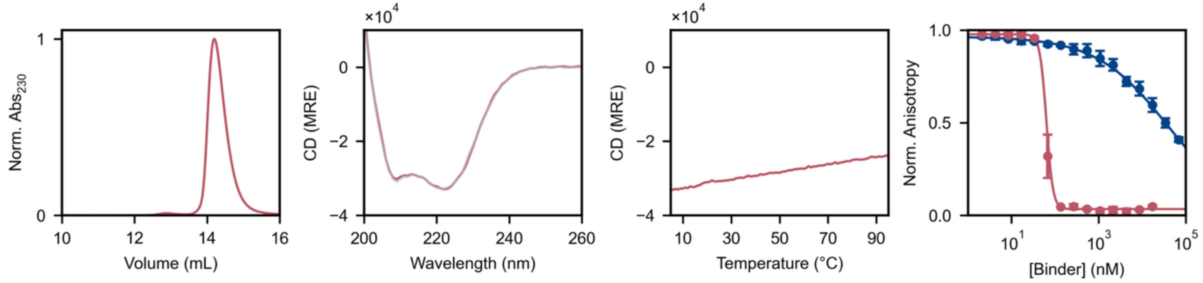

Sc-apCC-2-MCL-1-4

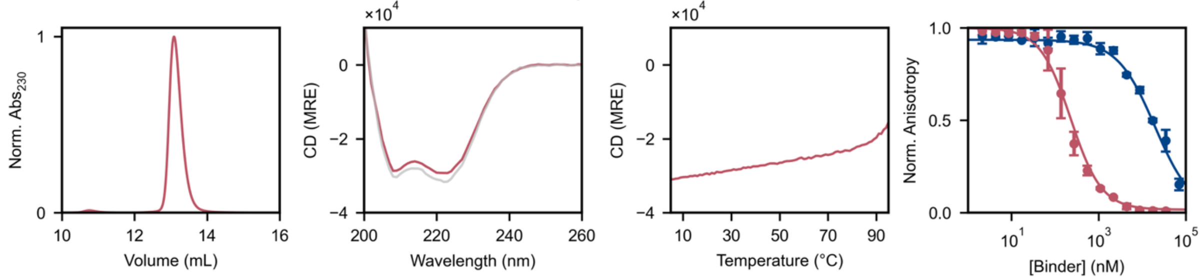

Sc-apCC-2-BCL-x$_L$-1

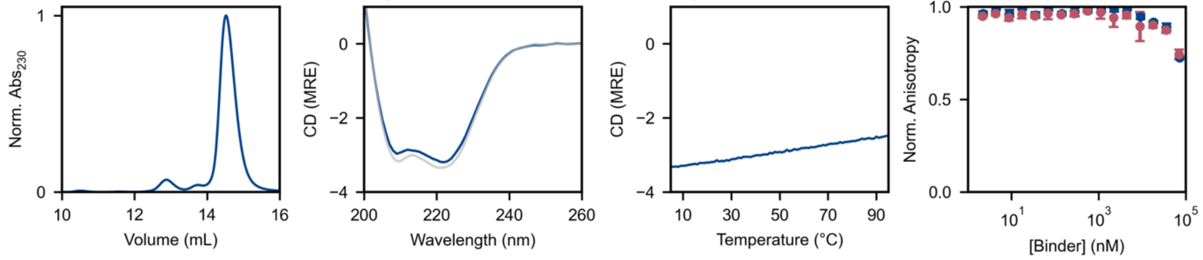

Sc-apCC-2-BCL-x$_L$-2

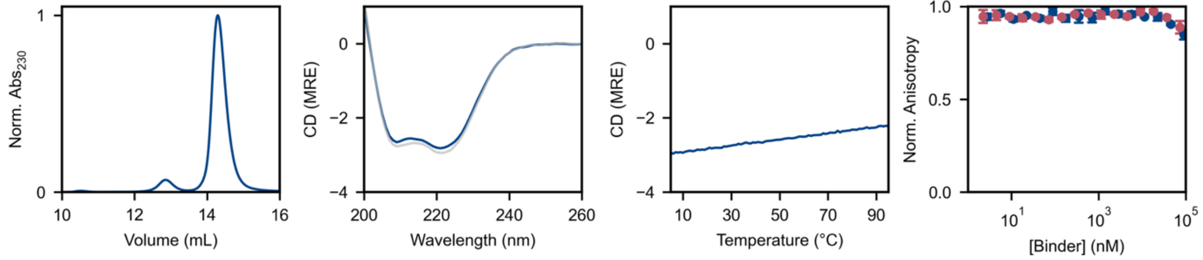

Sc-apCC-2-BCL-x_L-3

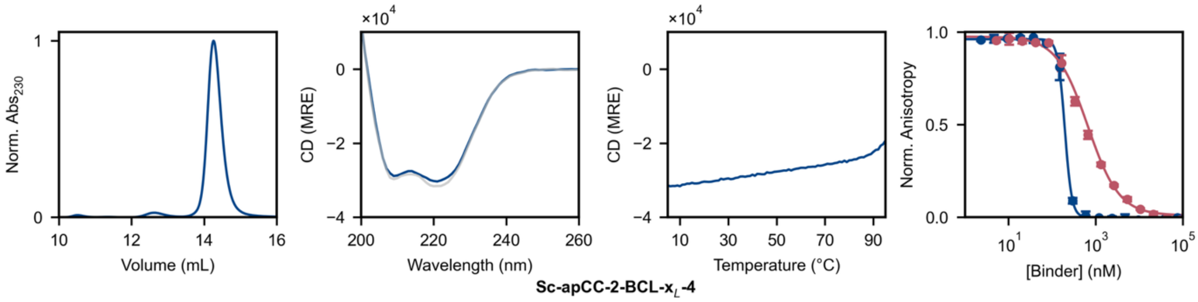

Sc-apCC-2-BCL-x_L-4

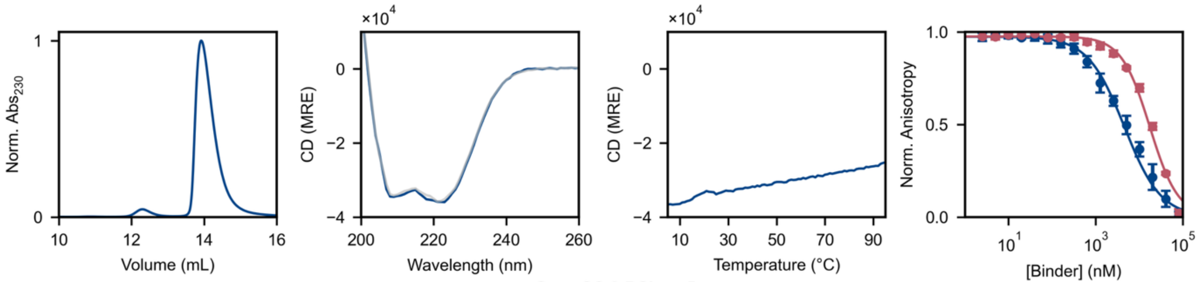

Sc-apCC-2-BCL-x_L-5

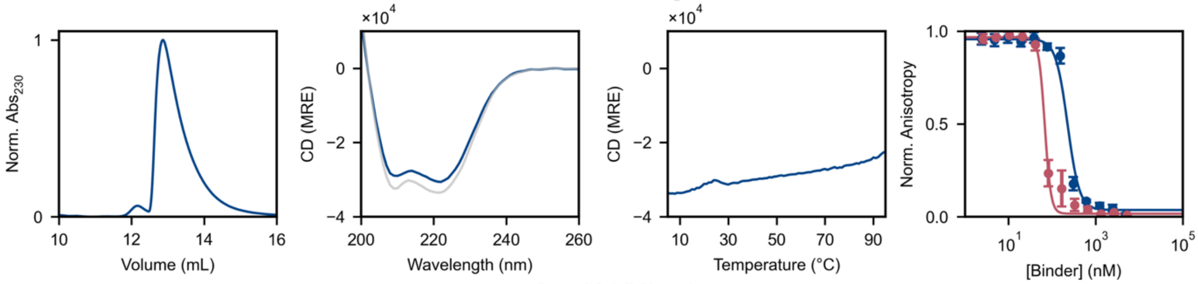

Sc-apCC-2-BCL-x_L-6

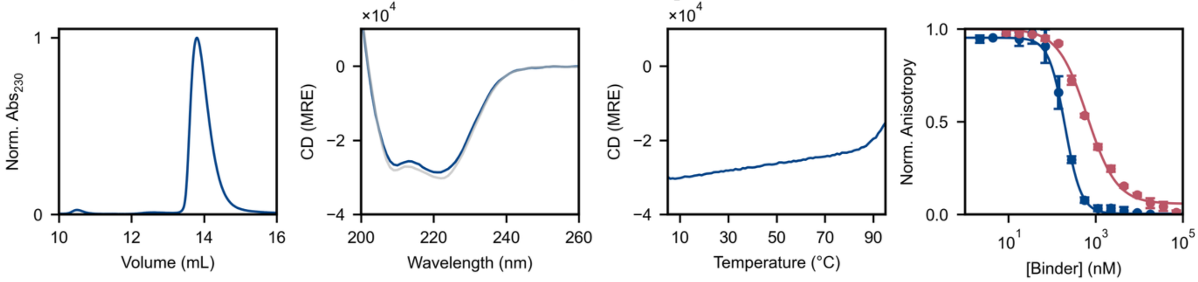

Sc-apCC-2-BCL-x_L-7

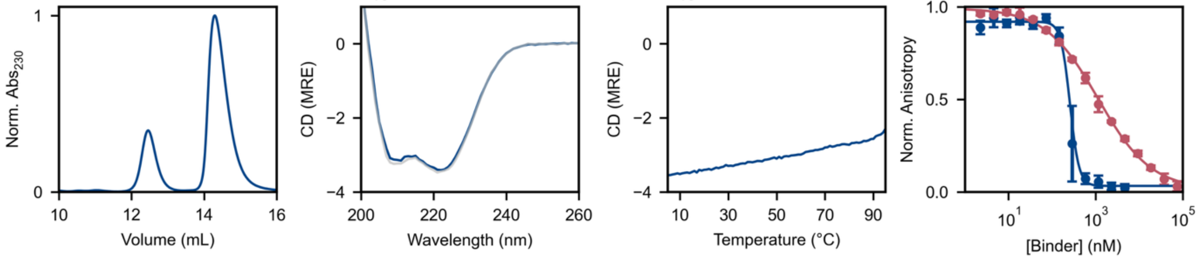

Sc-apCC-2-BCL-x_L-8

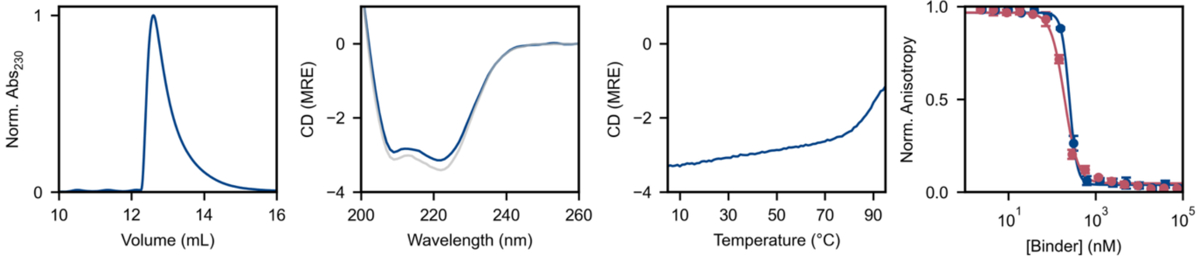

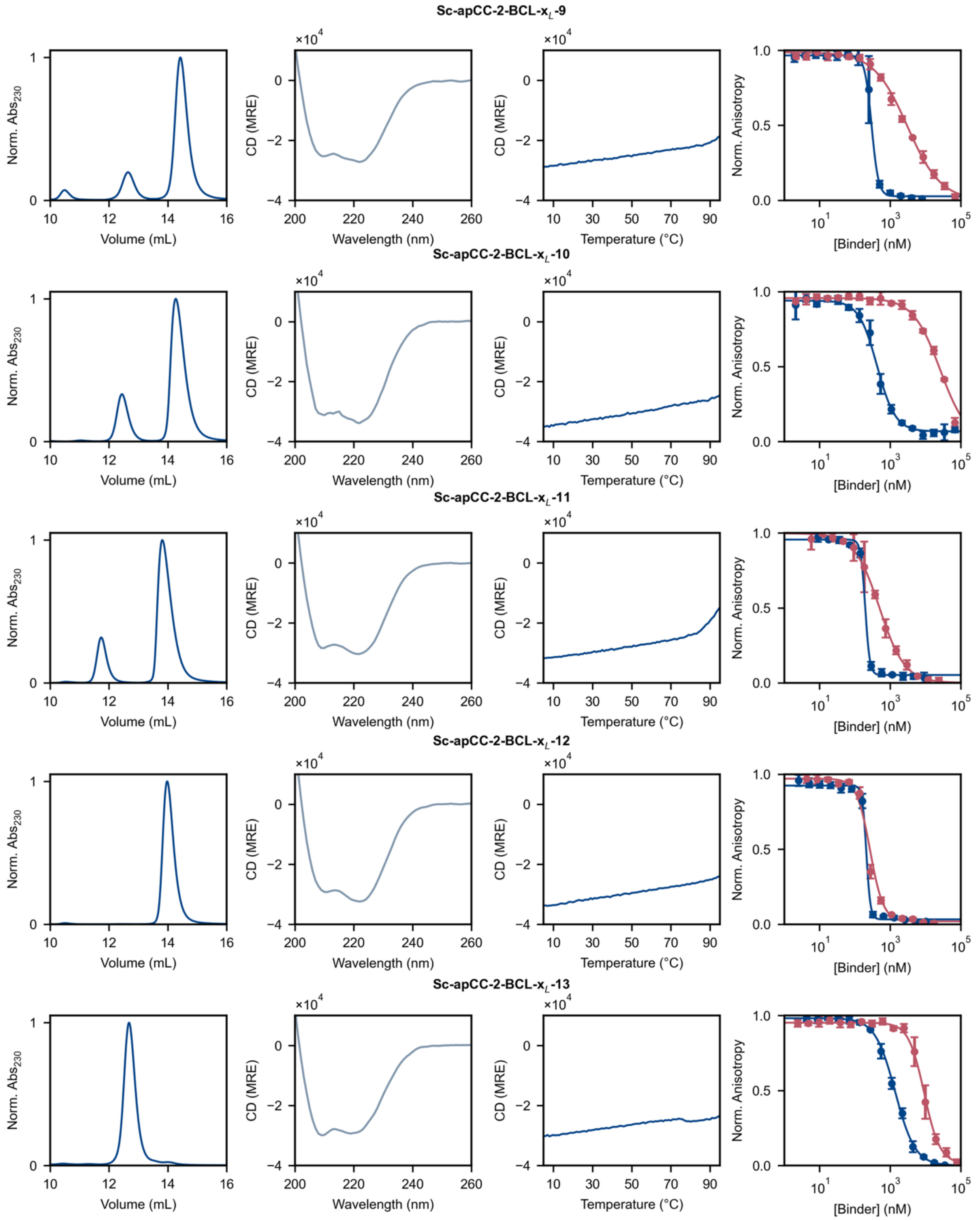

Supplementary Figure 3. Biophysics and fluorescent anisotropy data of the first round of designs. From left to right analytical size exclusion chromatography Superdex 75 increase, signal is shown as normalized UV absorbance at 230 nm; protein concentration 100 µM in 20 mM Tris-HCl, 150 mM NaCl, pH 7.5. CD spectrum; CD thermal melt; protein concentration 20 µM in 20 mM Tris-HCl, 150 mM NaCl, pH 7.5 FA assay against BCL-x$_L$ (dark blue) and MCL-1 (red) in 20 mM Tris-HCl, 150 mM NaCl, pH 7.5.

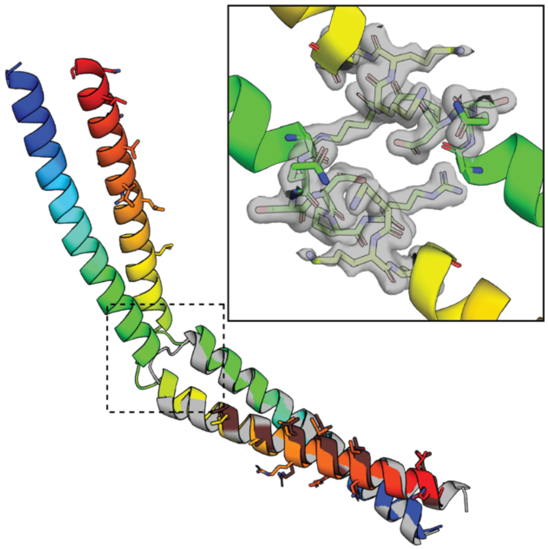

Supplementary Figure 4. Crystal structure of Sc-apCC-2-MCL-1-1. This crystal structure showed a domain-swapped dimer structure as opposed to the designed hairpin. Zoom-in shows electron density at sigma level 1 (PDB id 9TLM).

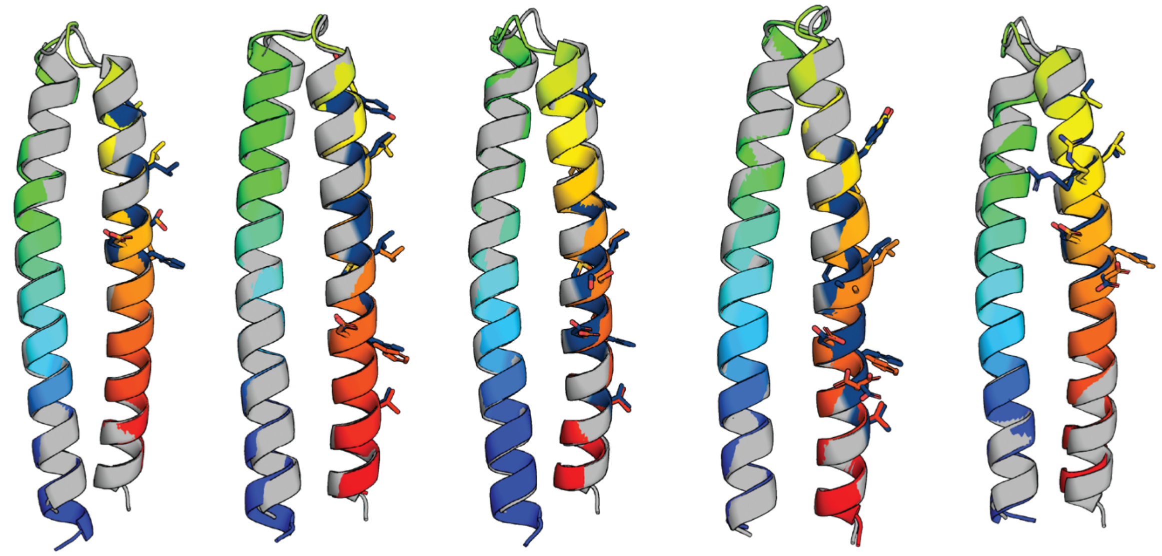

Sc-apCC-2-BCL-x$_L$-2 Sc-apCC-2-BCL-x$_L$-5 Sc-apCC-2-BCL-x$_L$-6 Sc-apCC-2-BCL-x$_L$-8 Sc-apCC-2-BCL-x$_L$-11

Supplementary Figure 5. Crystal structures of BCL-x$_L$ designs. (PDB ids 9TLN, 9TLO, 9TLQ, 9TLR)

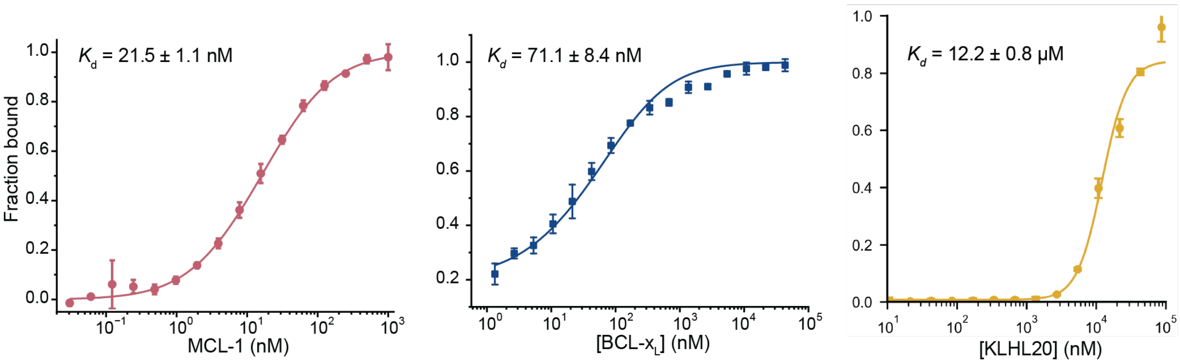

Supplementary Figure 6 Fluorescence anisotropy assay of direct titration of tracers. From left to right BID against MCL-1 (red), BID against BCL-x_L (dark blue) and DAPK1 against KLHL20 (yellow)

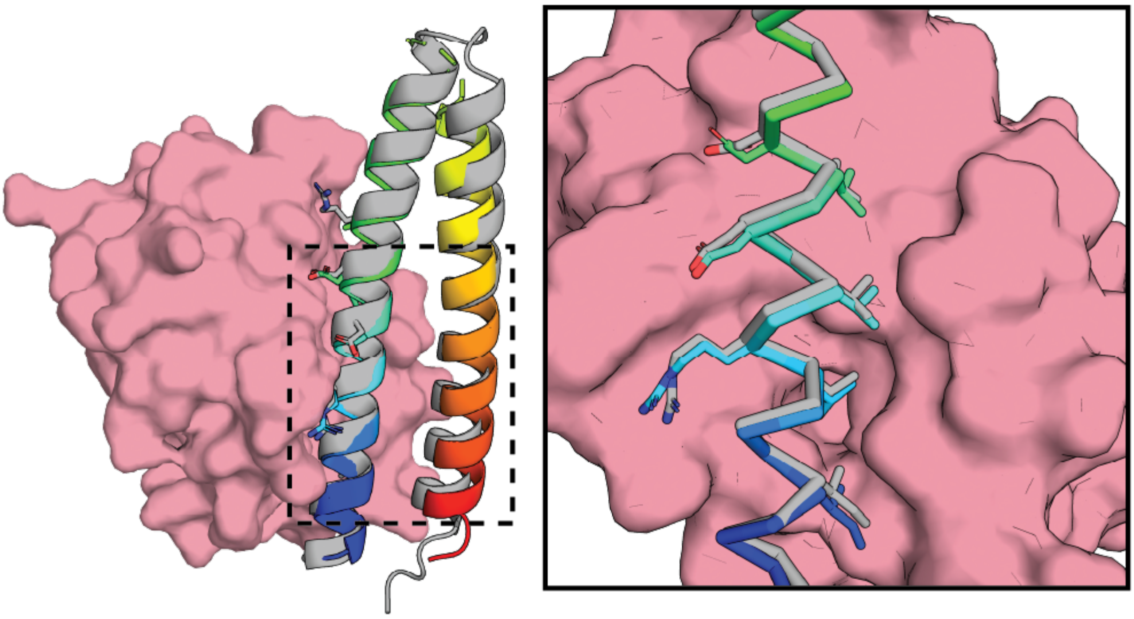

Supplementary Figure 7. Crystal structures of Sc-apCC-2-MCL-1-4 in complex with MCL-1. (PDB id 9TLW)

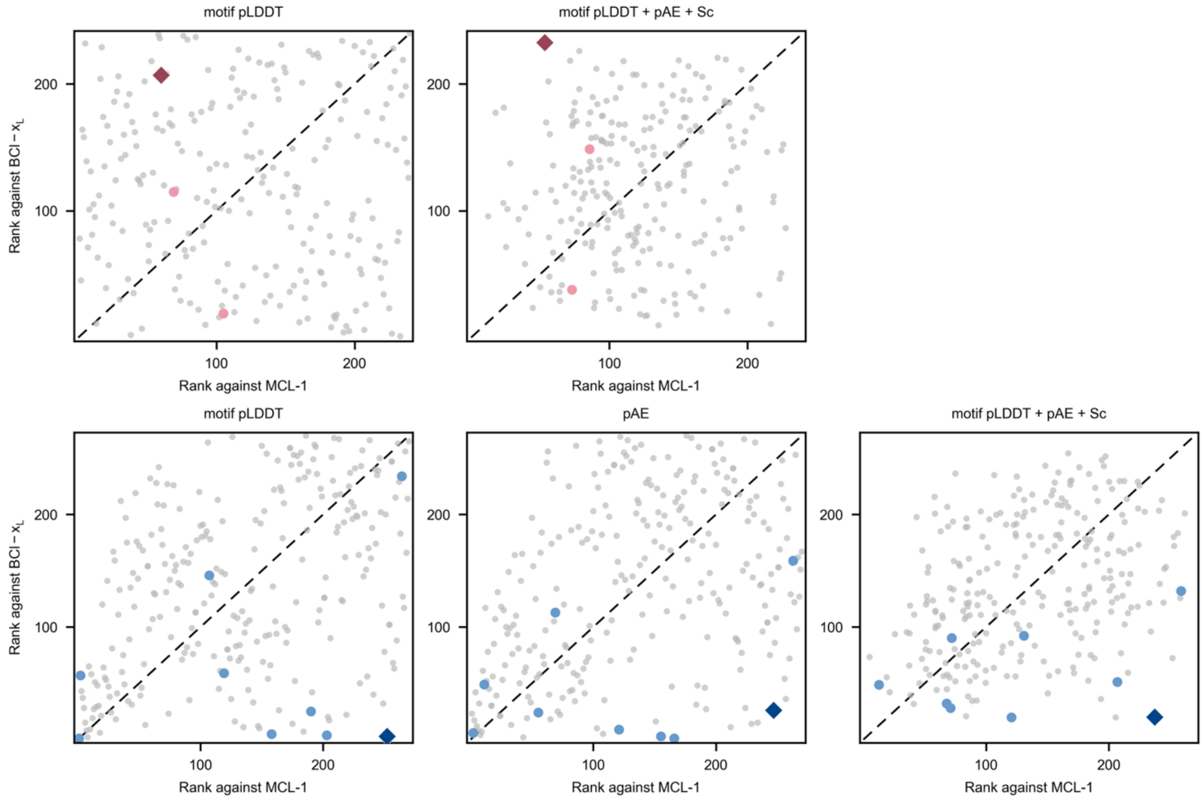

Supplementary Figure 8. Selectivity scatterplots for MCL-1 and BCL-x$_L$ selective designs. Each grey dot represents a single computational designed sequence. Its y-axis position is determined by its rank in a selected metric against BCL-x$_L$, and its x-axis position by the rank against MCL-1. The selected metric is shown as the title. The coloured dots represent sequences selected in the first design round. The diamond represents the sequence selected based on this metric.

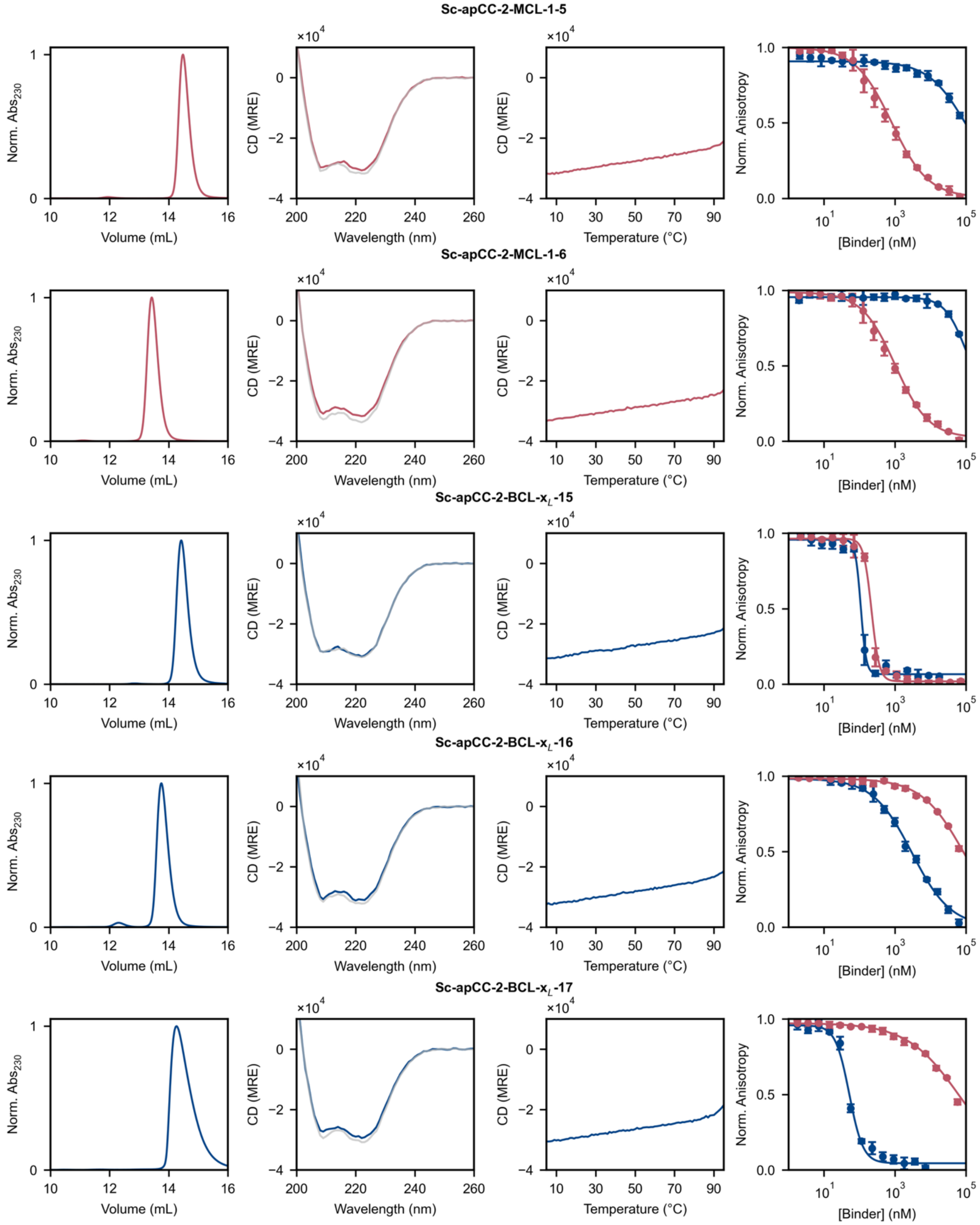

Supplementary Figure 9. Biophysics and fluorescent anisotropy data of designs selected for specificity. From left to right analytical size exclusion chromatography Superdex 75 increase, signal is shown as normalized UV absorbance at 230 nm; protein concentration 100 μM in 20 mM Tris-HCl, 150 mM NaCl, pH 7.5. CD spectrum; CD thermal melt; protein concentration 20 μM in 20 mM Tris-HCl, 150 mM NaCl, pH 7.5 FA assay against BCL-x$_L$ (dark blue) and MCL-1 (red) in 20 mM Tris-HCl, 150 mM NaCl, pH 7.5.

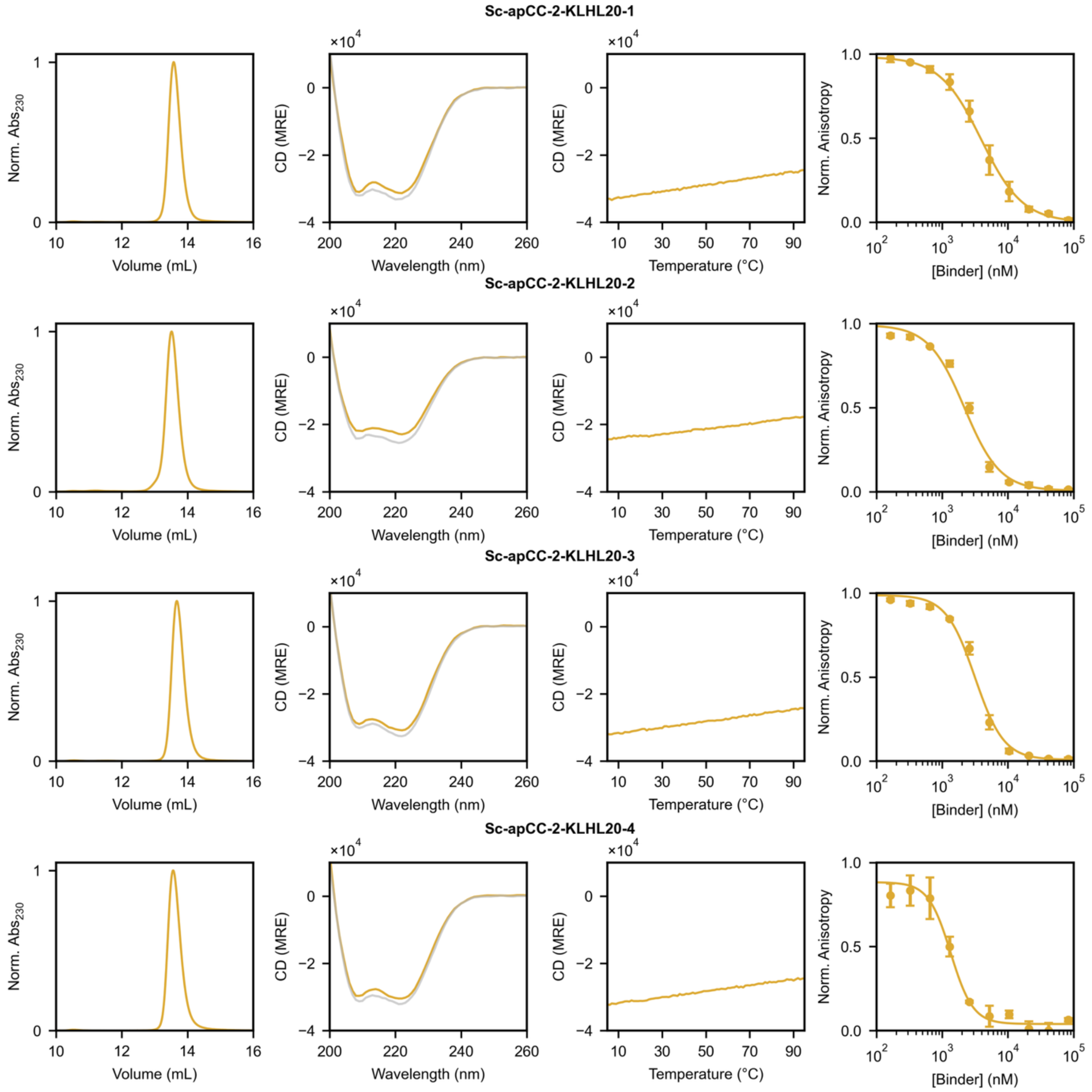

Supplementary Figure 10. Biophysics and fluorescent anisotropy data of designs against KLHL20. From left to right analytical size exclusion chromatography Superdex 75 increase, signal is shown as normalized UV absorbance at 230 nm; protein concentration 100 μM in 20 mM Tris-HCl, 150 mM NaCl, pH 7.5. CD spectrum; CD thermal melt; protein concentration 20 μM in 20 mM Tris-HCl, 150 mM NaCl, pH 7.5. FA assay against KLHL20 in 20 mM Tris-HCl, 150 mM NaCl, pH 7.5

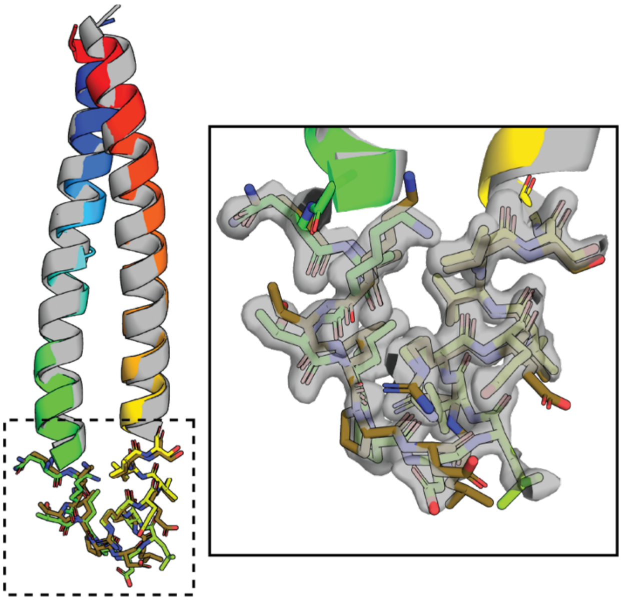

Supplementary Figure 11. Crystal structure of Sc-apCC-2-KLHL20-4. Zoom in shows electron density around the designed loop at sigma level 1 (PDB id 9TLT).

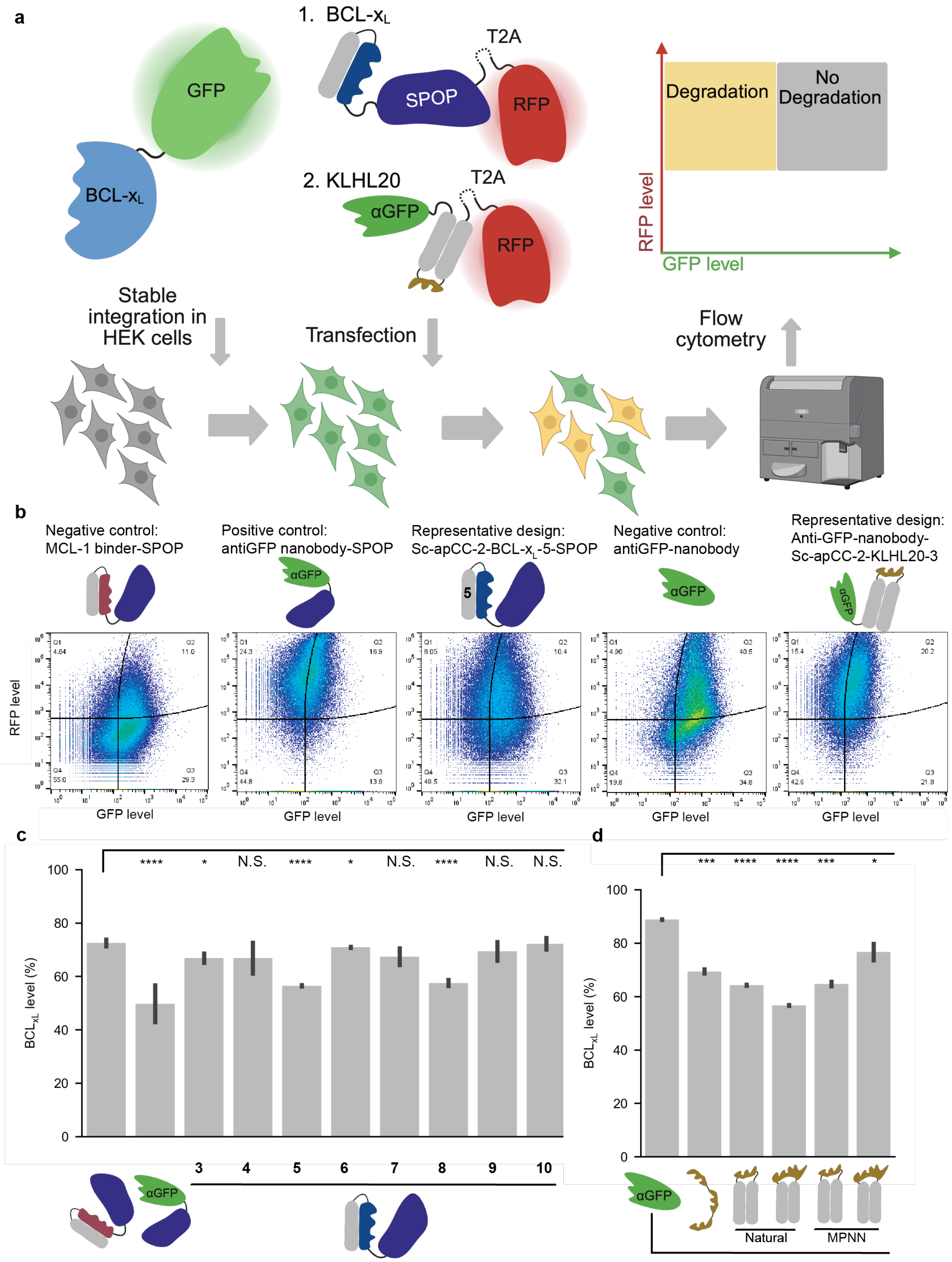

Supplementary Figure 12. Degradation assay of BCL-xL-GFP with BCL-x$_L$ binders and KLHL20 binders. a, Scheme of the GFP based assay, HEK293 cells were engineered to express BCL-x$_L$-GFP fusion proteins under an inducible promotor. Afterwards the cells were transfected either with fusion proteins consisting of the E3 ligase SPOP and a BCL-x$_L$ binder design with an RFP present after a self-cleaving T2A sequence, or fusions of an anti-GFP nanobody and a KLHL20 binding design with the same RFP sequence. These cells are subsequently measured in a flow cytometer. An increase in RFP signals expression of the degrader while decrease of GFP corresponds to success. **b,** 2D dot plots of representative measurements. From left to right negative control (Sc-apCC-2-MCL-1-1-SPOP), positive control (αGFP-SPOP), Sc-apCC-2-BCL-x$_L$-5-SPOP, negative control KLHL20 experiment (αGFP), αGFP-Sc-apCC-2-KLHL20-3. **c,** Histograms of BCL-x$_L$ designs, y-axis shows the level of BCL-x$_L$ calculated as 100 x Q2/(Q1 +Q2). Significance against the negative control was calculated by a two-sided Welch T-test. **d,** Histograms KLHL20 designs, y-axis shows the same calculated BCL-x$_L$ level. Significance levels were calculated with a two-sided Welch T-test against the negative control. Significance levels are represented as N.S.: $P > 0.05$, $*$: $P \leq 0.05$, $**$: $P \leq 0.01$, $***$: $P \leq 0.001$, $****$: $P \leq 0.0001$. The list of all used constructs is shown in table 8. Parts of this figure were made with BioRender.

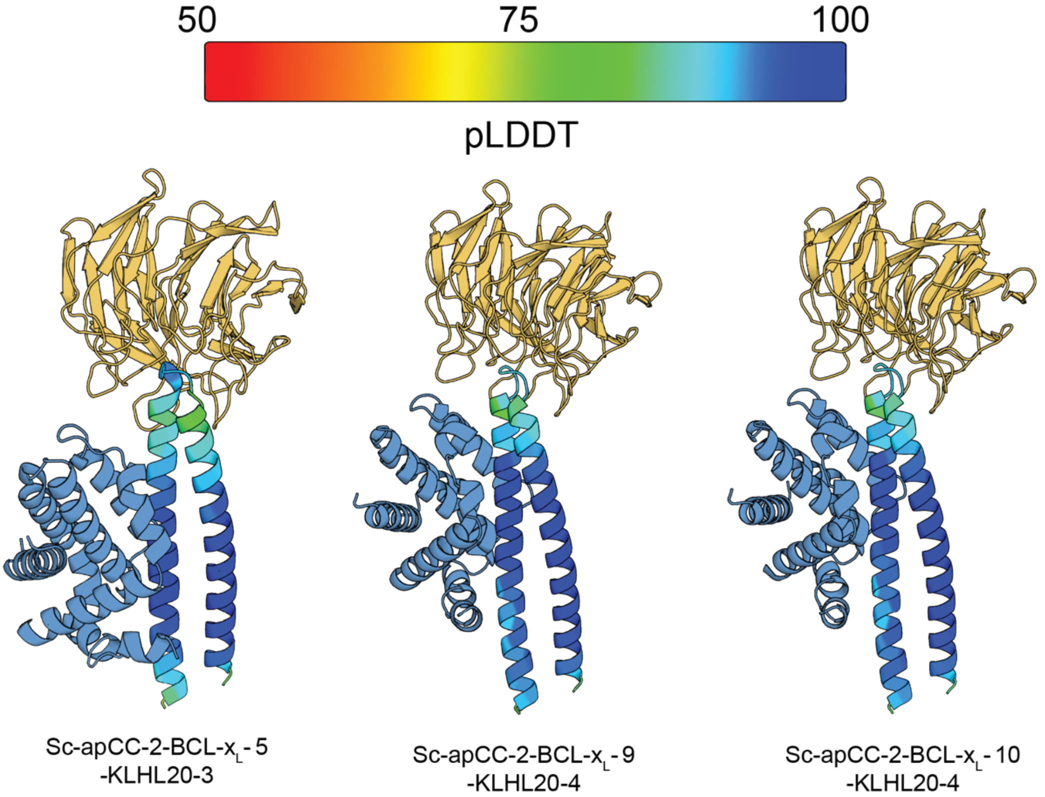

Supplementary Figure 13. Predicted ternary complexes of bifunctional binders. AlphaFold2 models of the ternary complexes between BCL-x$_L$ (blue), KLHL20 (yellow) and the bifunctional binders used. The binders are coloured according to AlphaFold2 pLDDT scores following the colorbar shown on top.

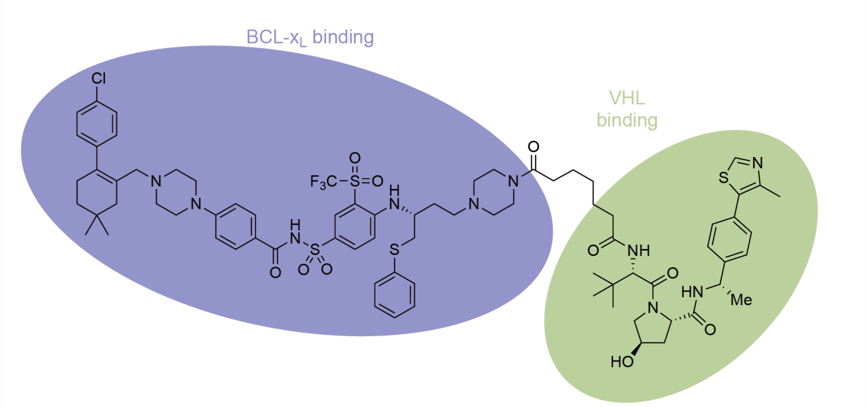

Supplementary Figure 14. Chemical structure of DT2216

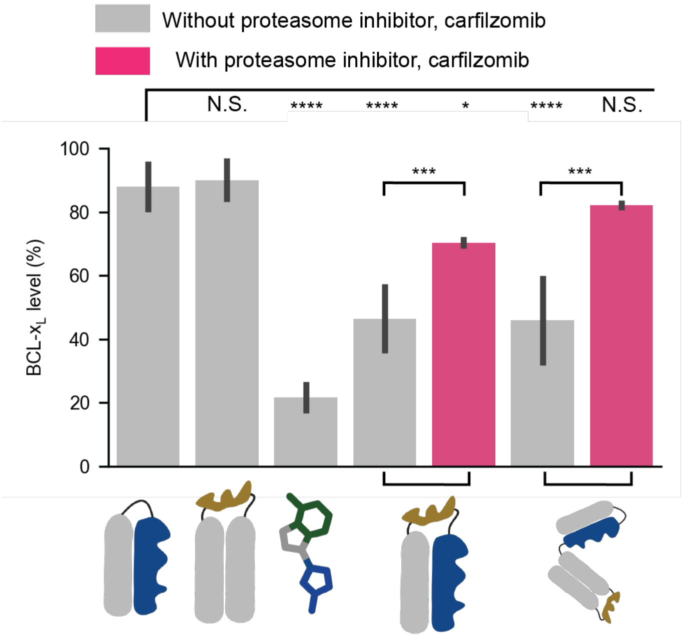

Supplementary Figure 15. Endogenous degradation with carfilzomib as proteasome inhibitor. Histograms showing BCL-x$_L$ degradation in the A549 cell line. From left to right: the monofunctional controls, Sc-apCC-2-BCL-x$_L$-5, Sc-apCC-2-KLHL20-3, DT2216 as positive control, bifunctional hairpin Sc-apCC-2-BCL-x$_L$-5-KLHL20-3 and fusion construct of both monofunctional hairpins Sc-apCC-2-BCL-x$_L$-5_sc-apCC-2-KLHL20-3. The pink bars correspond to the tests with addition of the proteasome inhibitor. Significance levels calculated with a Welch t-test against the monofunctional BCL-x$_L$ binder shown on top. The significance level between the samples with and without the inhibitor was also calculated with a Welch T-test. Significance levels are represented as N.S.: $P > 0.05$, ∗: $P \leq 0.05$, ∗∗: $P \leq 0.01$, ∗∗∗: $P \leq 0.001$, ∗∗∗∗: $P \leq 0.0001$. Parts of this figure were made with BioRender.

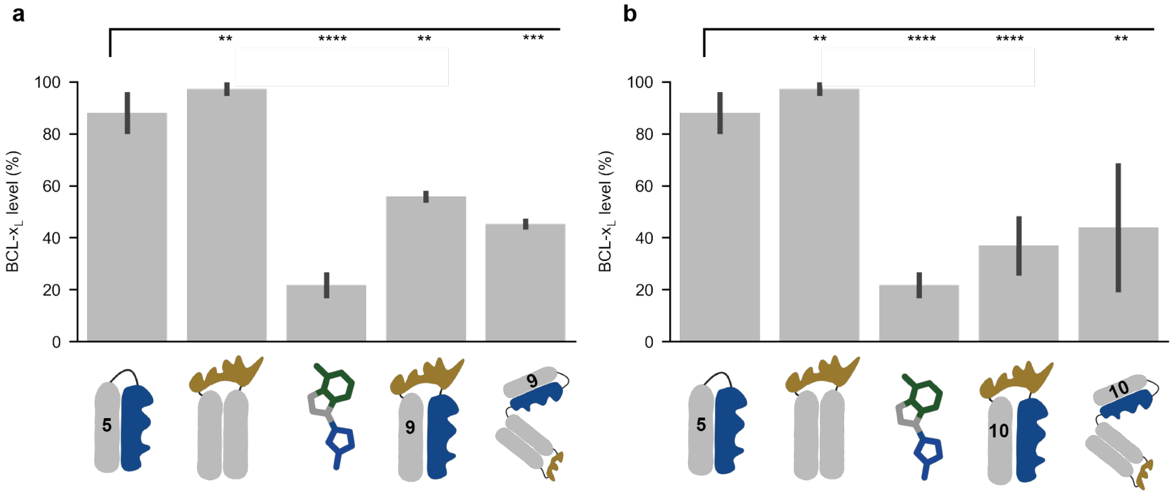

Supplementary Figure 16. Additional endogenous degradation constructs. Histograms showing BCL-x$_L$ degradation in the A549 cell line. **a,** constructs based on Sc-apCC-2-BCL-x$_L$-9 and Sc-apCC-2-KLHL20-3 **b,** constructs based on Sc-apCC-2-BCL-x$_L$-10 and Sc-apCC-2-KLHL20-4. Significance levels are represented as N.S.: $P > 0.05$, $*$: $P \leq 0.05$, $**$: $P \leq 0.01$, $***$: $P \leq 0.001$, $****$: $P \leq 0.0001$. Parts of this figure were made with BioRender.

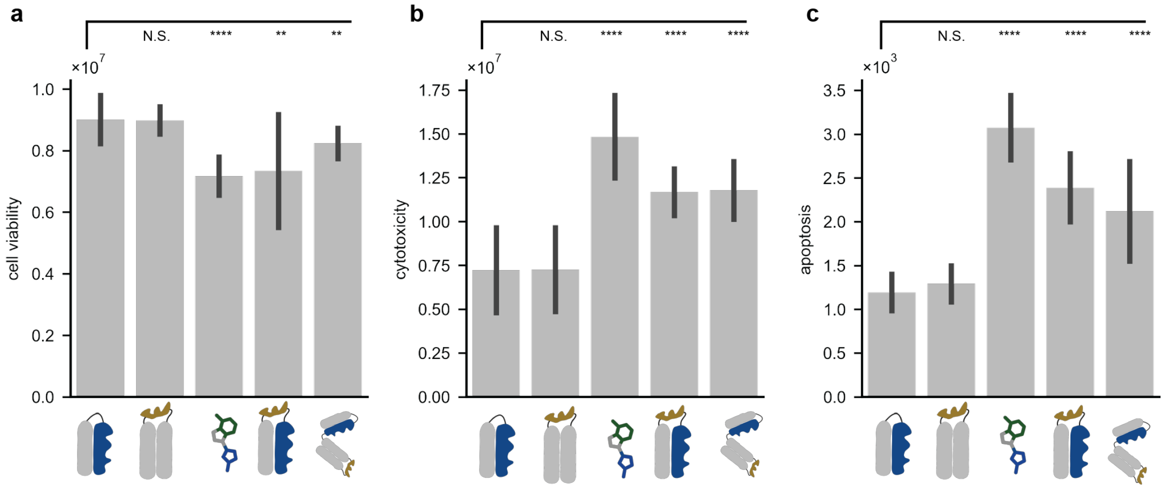

Supplementary Figure 17. ApoTox-Glo™ Triplex Assay with Sc-apCC-2-BCL-x$_L$-5-KLHL20-3 constructs. a, cell viability **b,** Cytotoxicity **c,** apoptosis. Significance levels are represented as N.S.: $P > 0.05$, $*$: $P \leq 0.05$, $**$: $P \leq 0.01$, $***$: $P \leq 0.001$, $****$: $P \leq 0.0001$. Parts of this figure were made with BioRender.

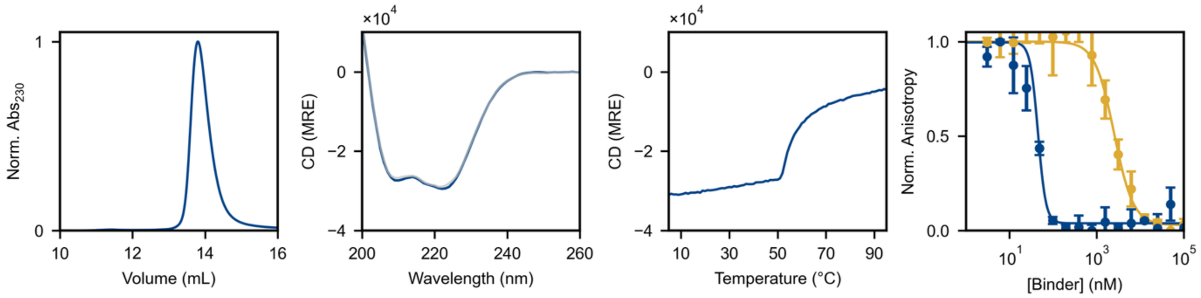

Supplementary Figure 18. Biophysics and fluorescent anisotropy data of bifunctional Sc-apCC-2-BCL-x$_L$-5-KLHL20-3. From left to right analytical size exclusion chromatography Superdex 75 increase, signal is shown as normalized UV absorbance at 230 nm; protein concentration 100 µM in 20 mM Tris-HCl, 150 mM NaCl, pH 7.5. CD spectrum; CD thermal melt; protein concentration 20 µM in 20 mM Tris-HCl, 150 mM NaCl, pH 7.5. FA assay against BCL-x$_L$ (dark blue) and KLHL20 (yellow) in 20 mM Tris-HCl, 150 mM NaCl, pH 7.5.

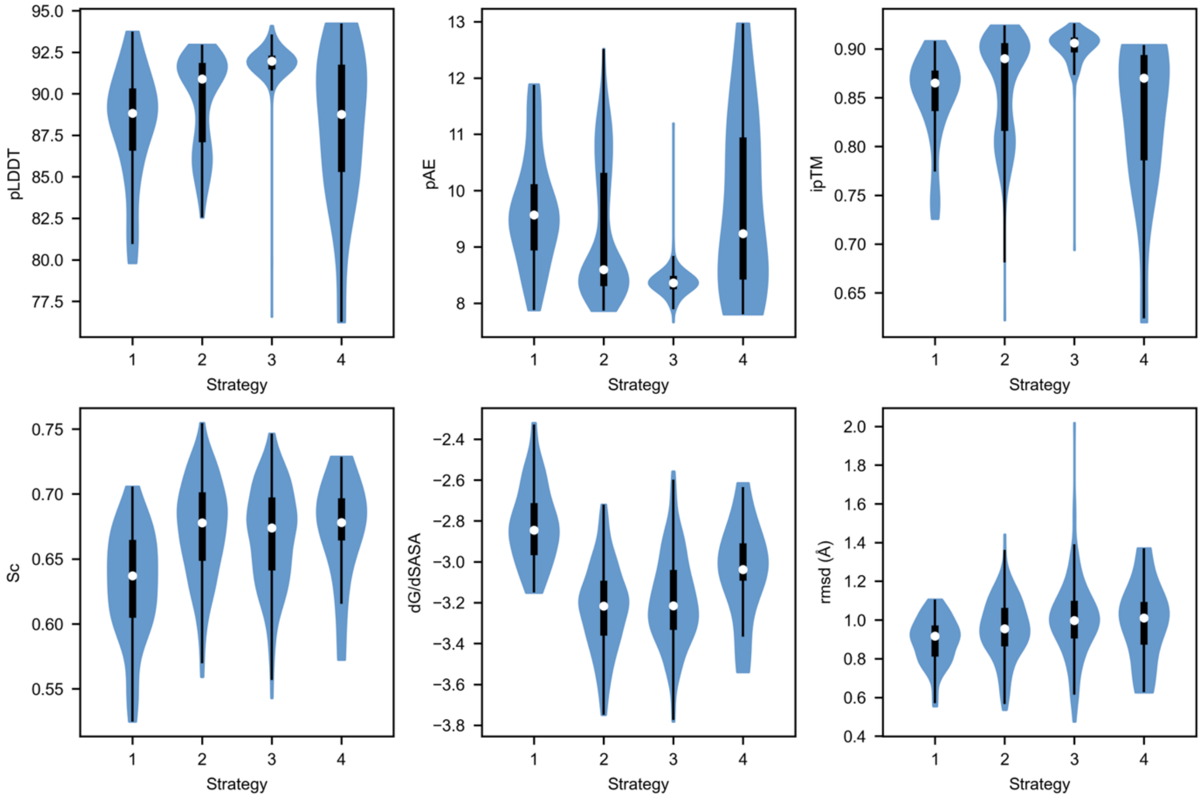

Supplementary Figure 19. Violin plots of *in silico* designed sequences against BCL-x$_L$ following the different implementation strategy of ProteinMPNN Strategy 1 no-additional MPNN; strategy 2, additional MPNN within 6 Å of target; strategy 3, MPNN at all non-critical positions; strategy 4, MPNN at all non-critical positions and altering motif

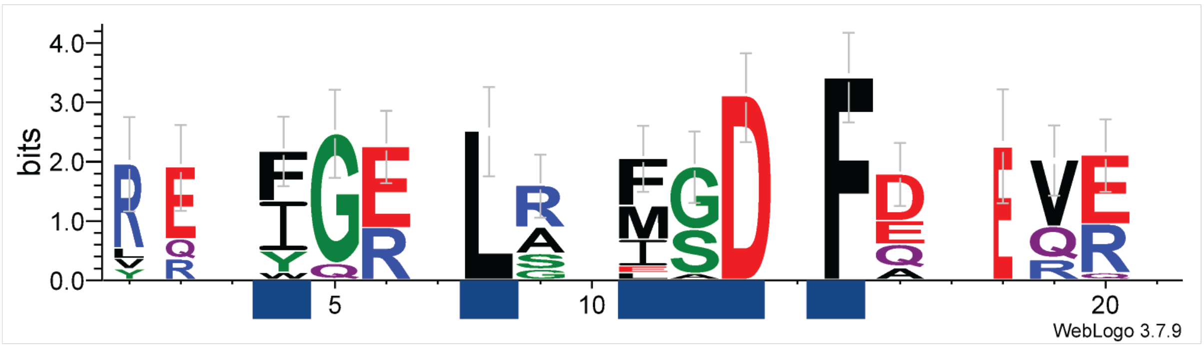

Supplementary Figure 20. Sequence logo of all experimentally tested designs against BCL-x$_L$. Blue boxes indicate motif positions. This weblogo was made with (https://weblogo.threeplusone.com)

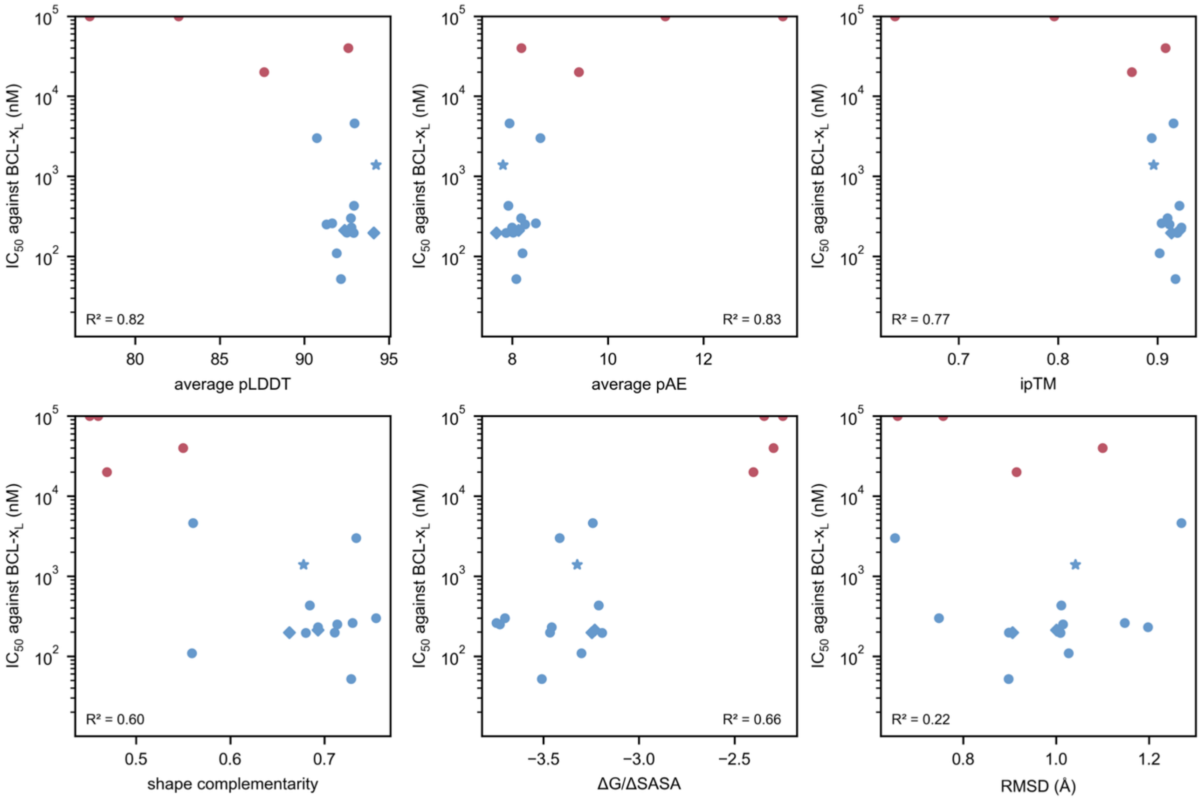

Supplementary Figure 21. Plots of measured IC$_{50}$ values against BCL-x$_L$ in function of *in silico* metrics. IC$_{50}$ are plotted on a logarithmic scale. R^2 value of a linear correlation is shown at the bottom. Red dots correspond to sequences designed against MCL-1; Blue dots correspond to sequences designed by strategy 2; blue diamonds correspond to sequences designed by strategy 3; blue star corresponds to sequences designed by strategy 4.

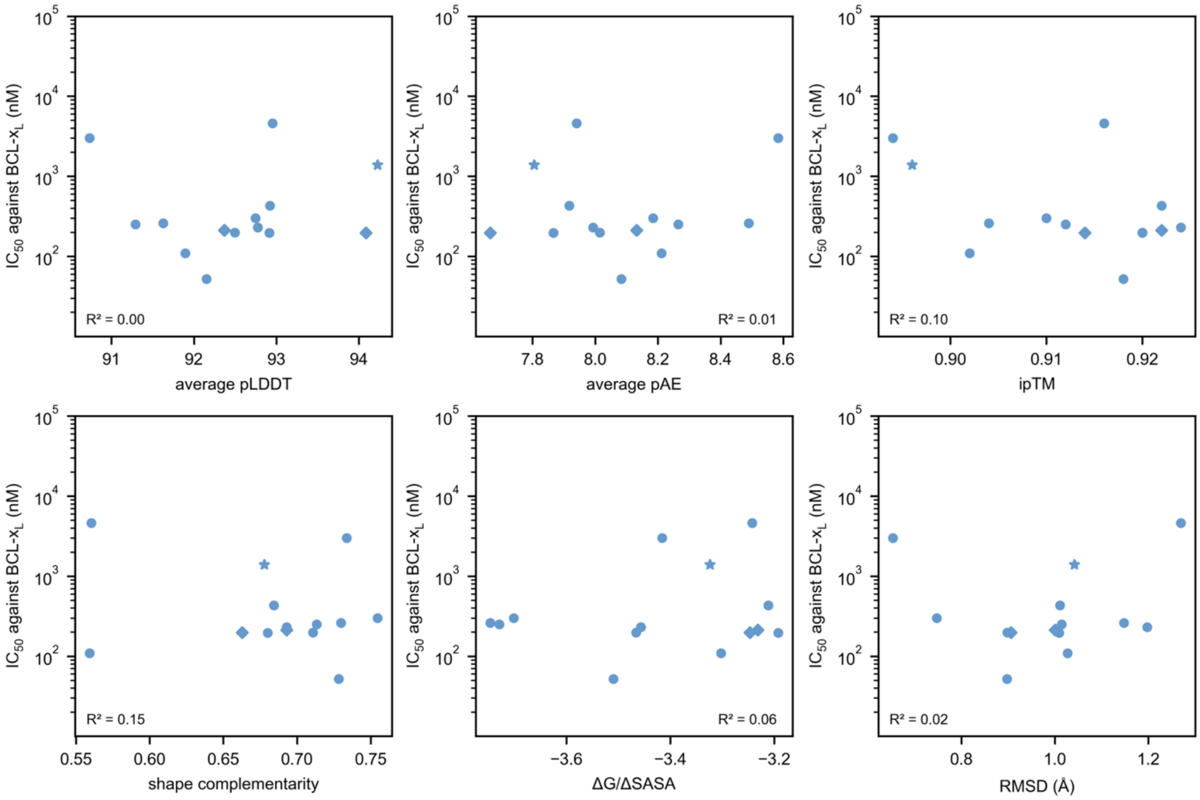

Supplementary Figure 22. Plots of measured IC$_{50}$ values against BCL-x$_L$ in function of *in silico* metrics. Same as in Figure 19 but without including the MCL-1 designs. IC$_{50}$ are plotted on a logarithmic scale. R^2 value of a linear correlation is shown at the bottom. Blue dots correspond to sequences designed by strategy 2; blue diamonds correspond to sequences designed by strategy 3; blue star corresponds to sequences designed by strategy 4.

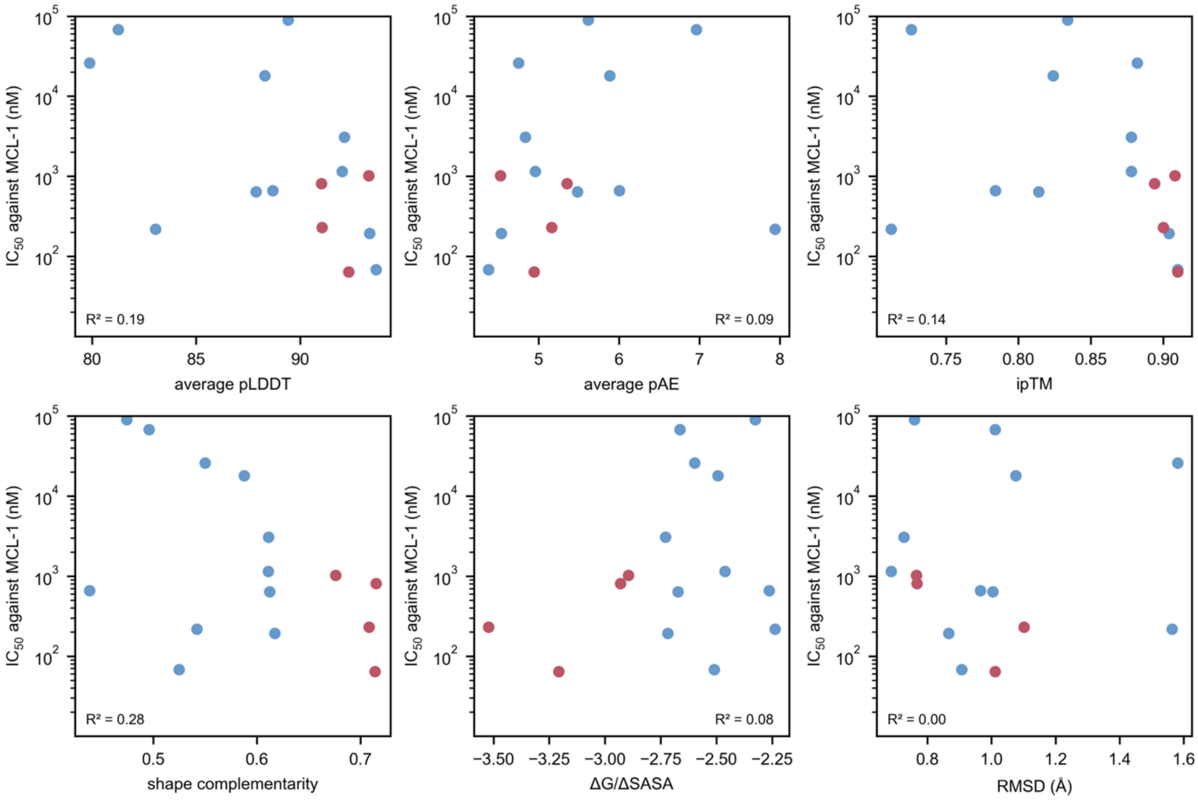

Supplementary Figure 23. Plots of measured IC_{50} values against MCL-1 in function of *in silico* metrics. IC_{50} are plotted on a logarithmic scale. R^2 value of a linear correlation is shown at the bottom. Red dots correspond to sequences designed against MCL-1; Blue dots correspond to sequences designed by strategy 2.

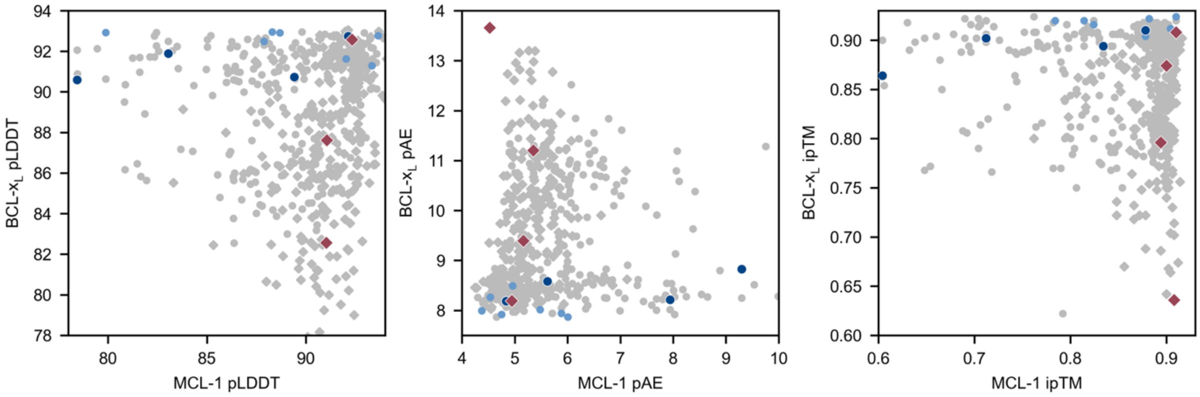

Supplementary Figure 24. Scatter plots of AlphaFold2 confidence metrics against MCL-1 and BCL-x_L. From left to right, pLDDT, pAE and ipTM. The sequences designed against BCL-x_L are shown as grey dots (not tested), light blue dots (non-specific designs) and dark blue dots (specific designs IC_{50} against MCL-1 < 10x IC_{50} against BCL-x_L). The sequences designed against MCL-1 are shown as grey diamond (not tested), and red diamond (specific designs)

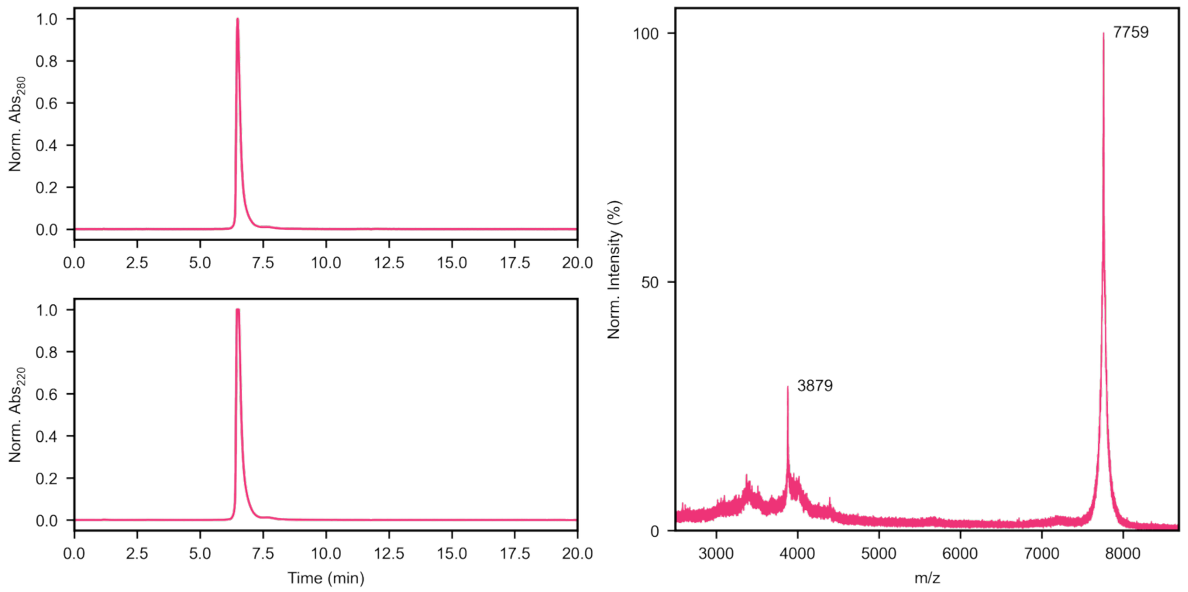

Supplementary Figure 25. Validation of Sc-apCC-2

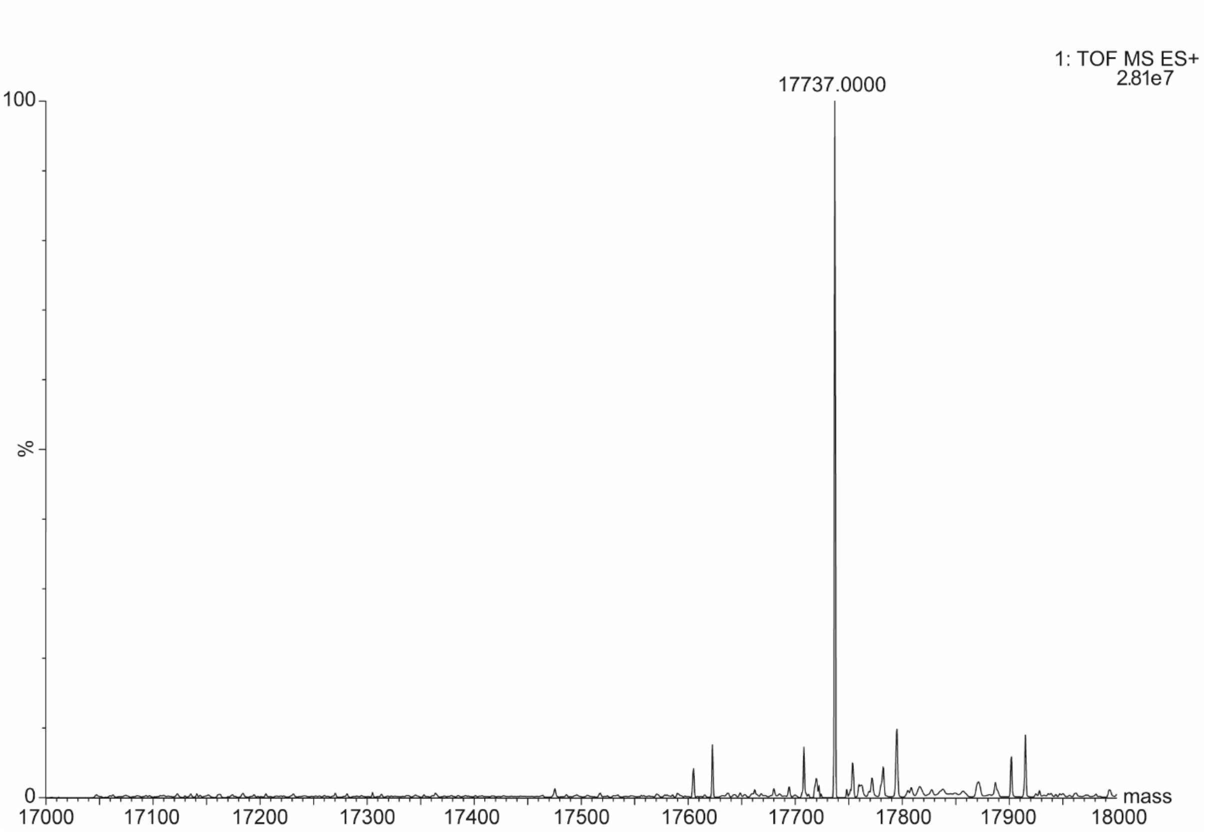

Supplementary Figure 26. Mass spectrometry of MCL-1. Predicted MW 17,737.2. Observed 17,737.0.

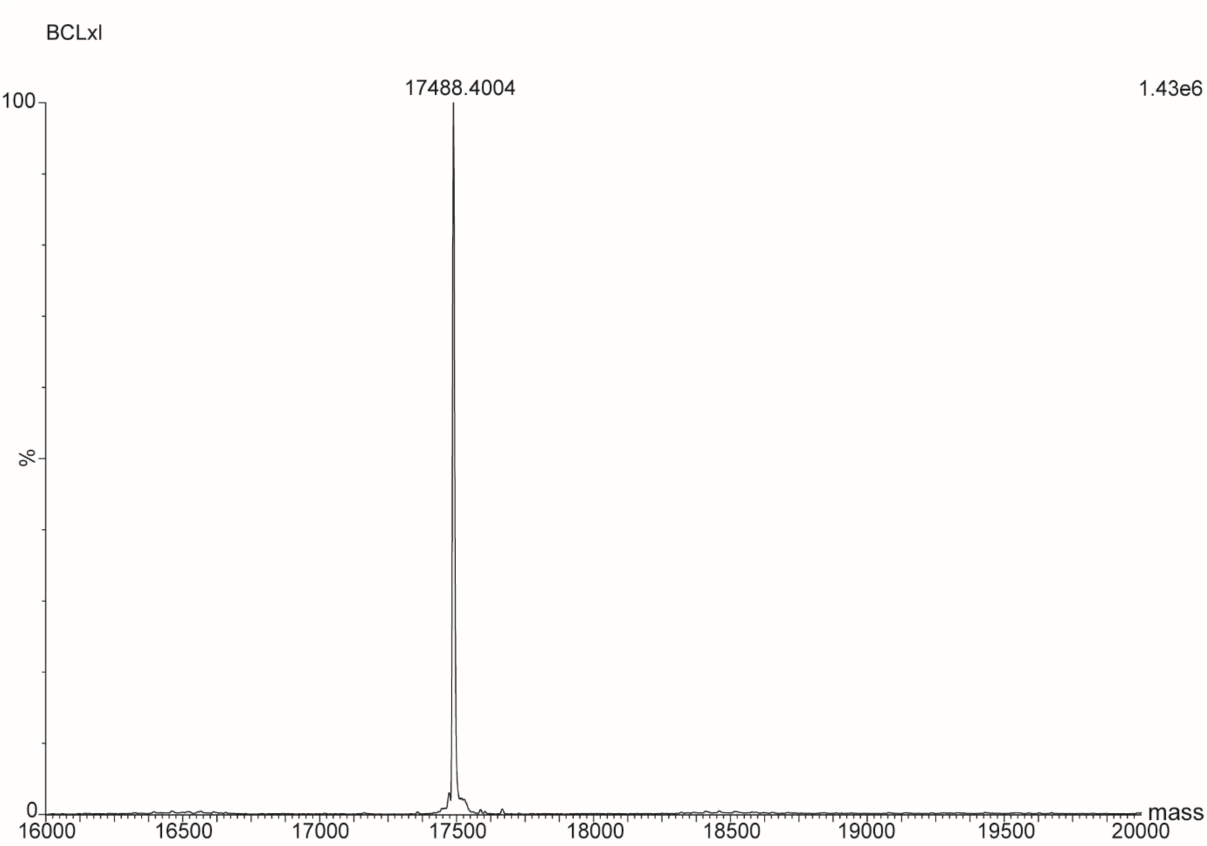

Supplementary Figure 27. Mass spectrometry result of BCL-x$_L$. Predicted 17,489.5. Observed 17488.4.

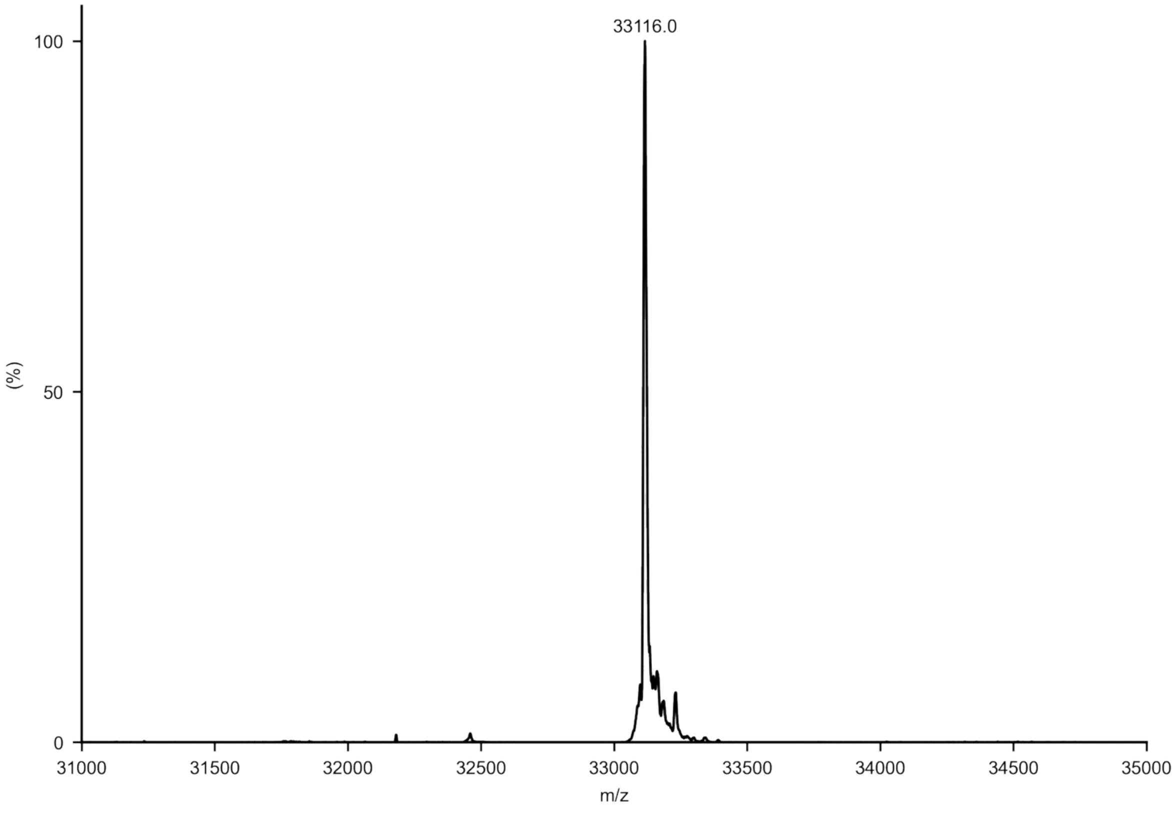

Supplementary Figure 28. Mass spectrometry result of KLHL20. Predicted 33117.0 Observed 33116.0

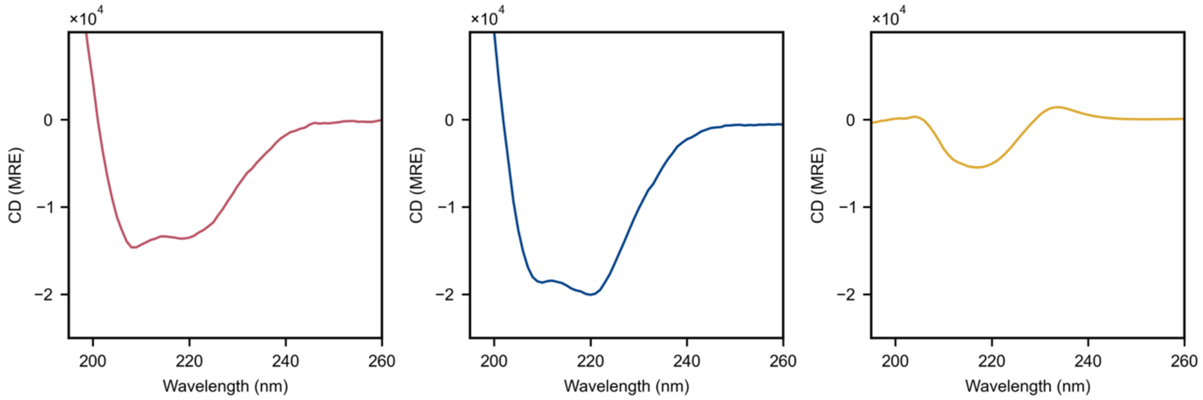

Supplementary Figure 29. CD spectrometry of binding targets. From left to right MCL-1 (red), BCL-x$_L$ (blue) and KLHL20 (yellow)

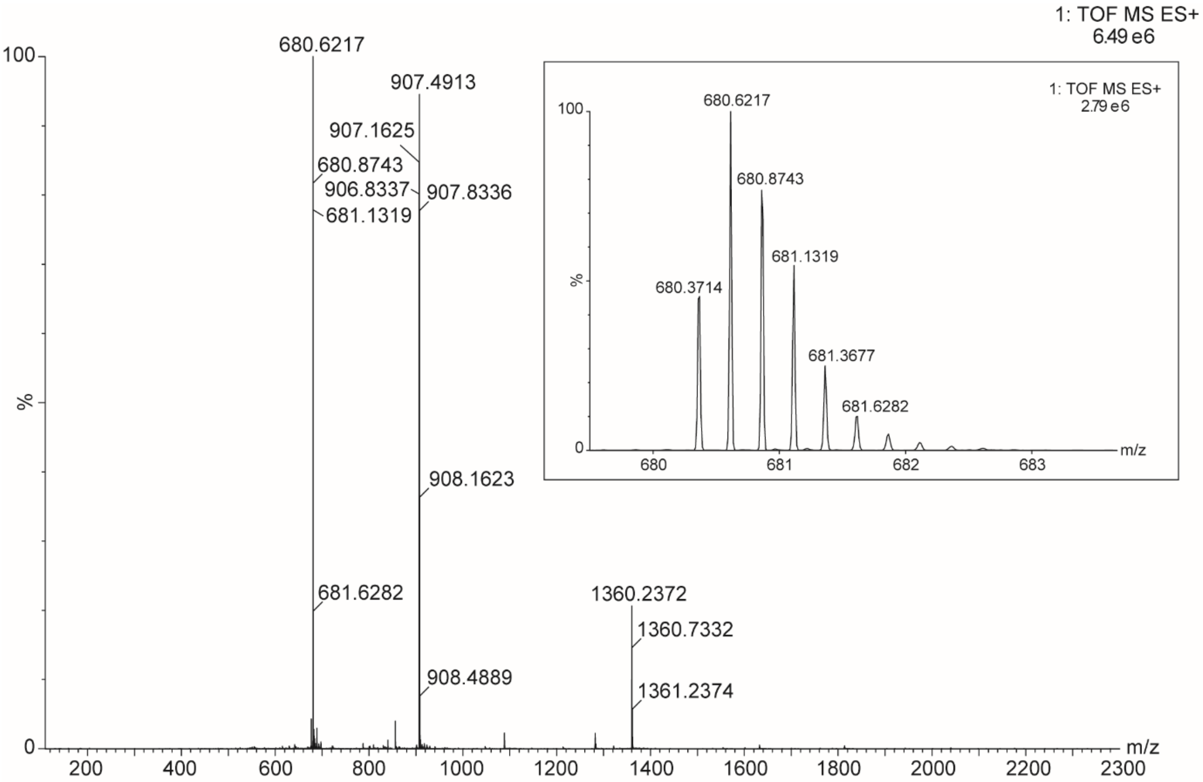

Supplementary Figure 30 Mass spectrometry result for BID. Predicted 2,717.441. Observed 2,717.446.

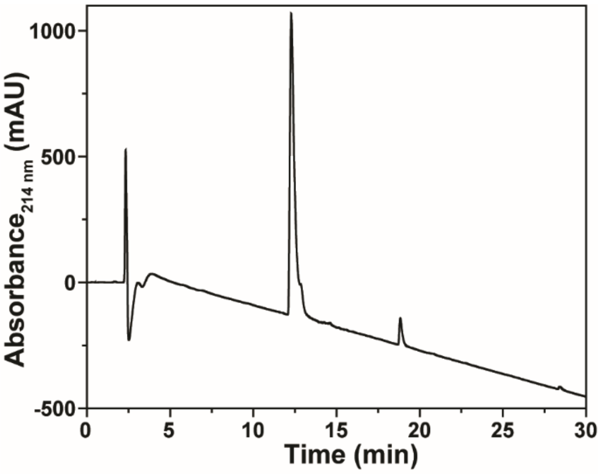

Supplementary Figure 31 Analytical HPLC result for BID.

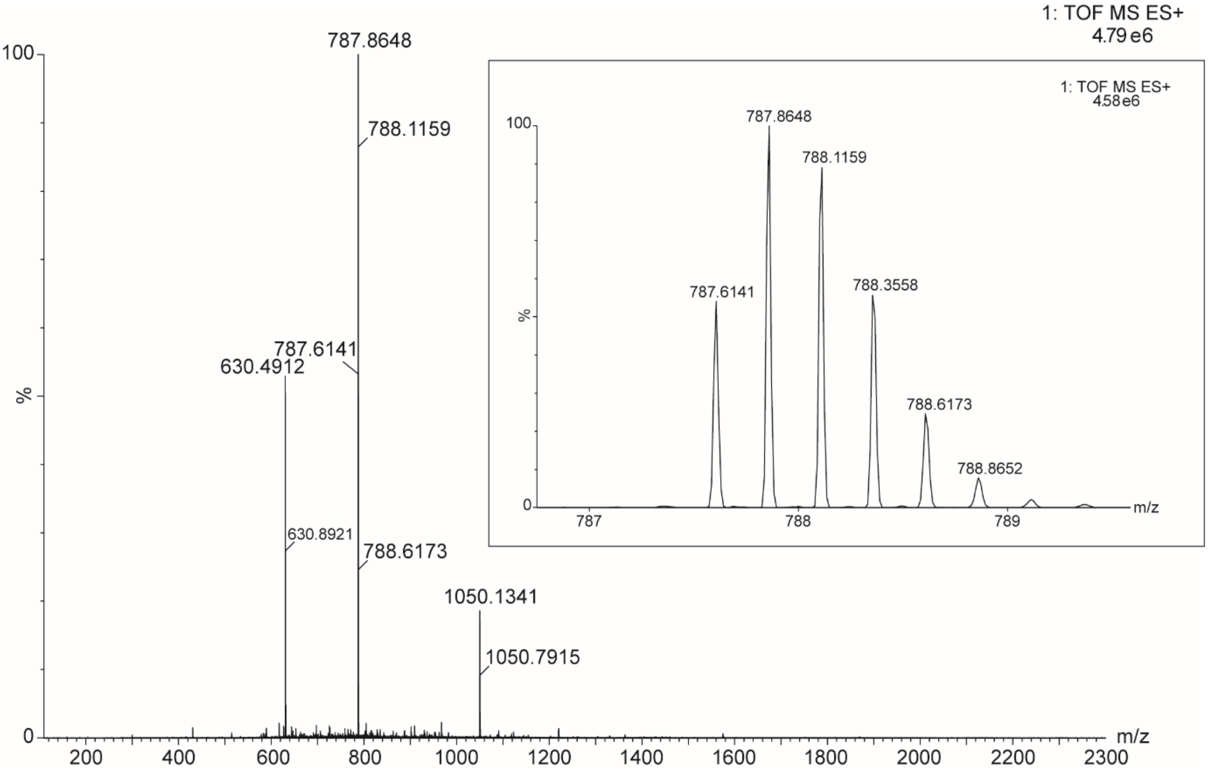

Supplementary Figure 32 Mass spectrometry result for FAM-BID Predicted 3,146.563. Observed 3,146.416.

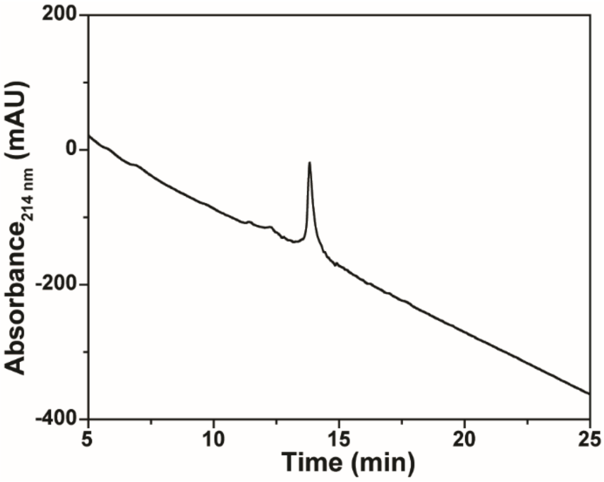

Supplementary Figure 33 Analytical HPLC result for FAM-BID

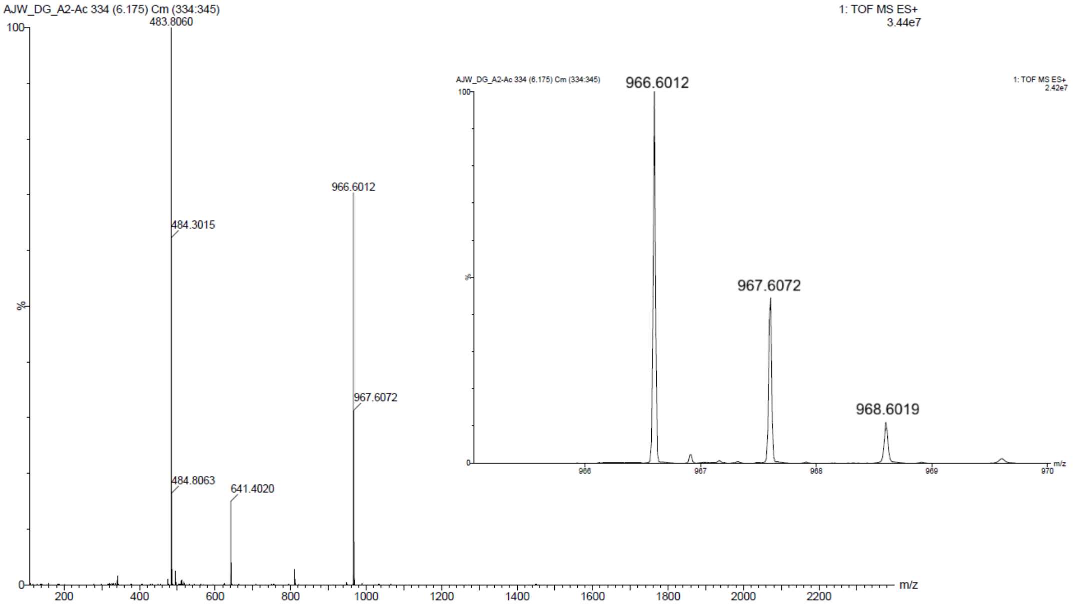

Supplementary Figure 34 Mass spectrometry result for DAPK1. Predicted 966.60 Observed 966.6

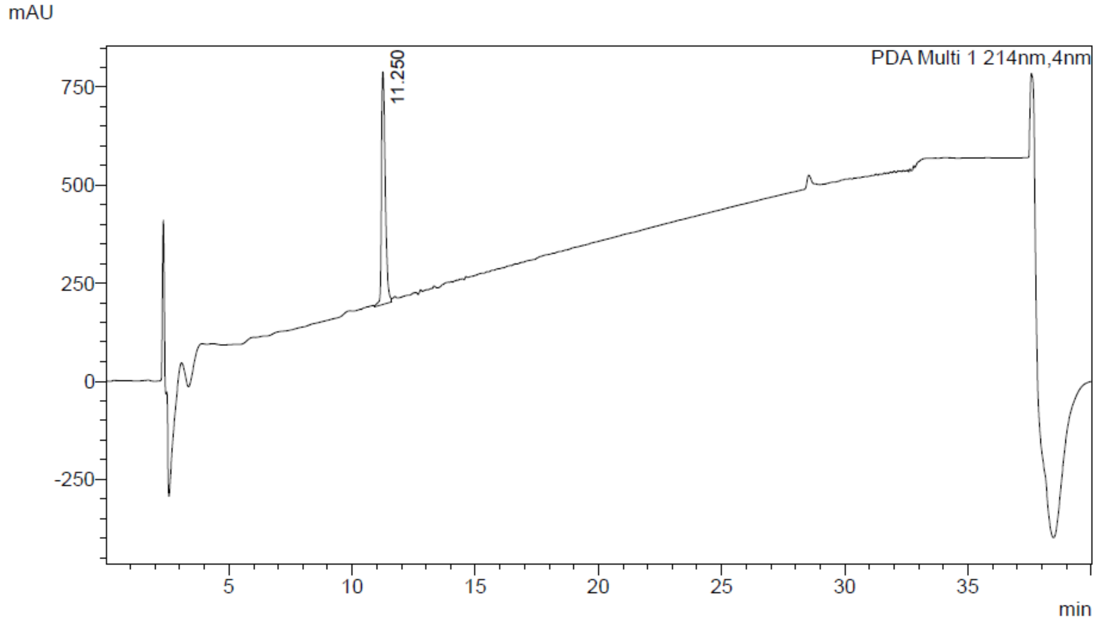

Supplementary Figure 35 Analytical HPLC result for DAPK1.

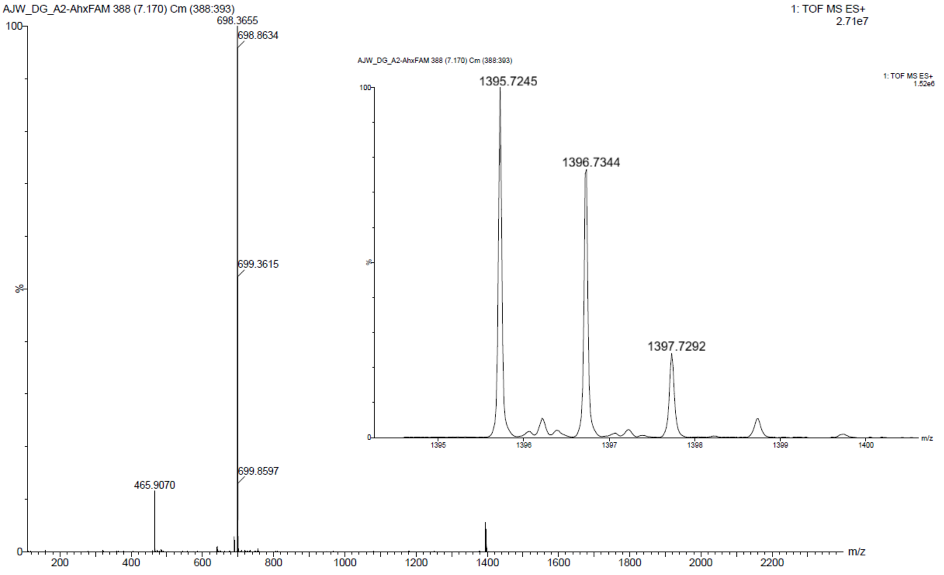

Supplementary Figure 36 Mass spectrometry result for FAM-DAPK1. Predicted 1395.72 Observed 1395.72

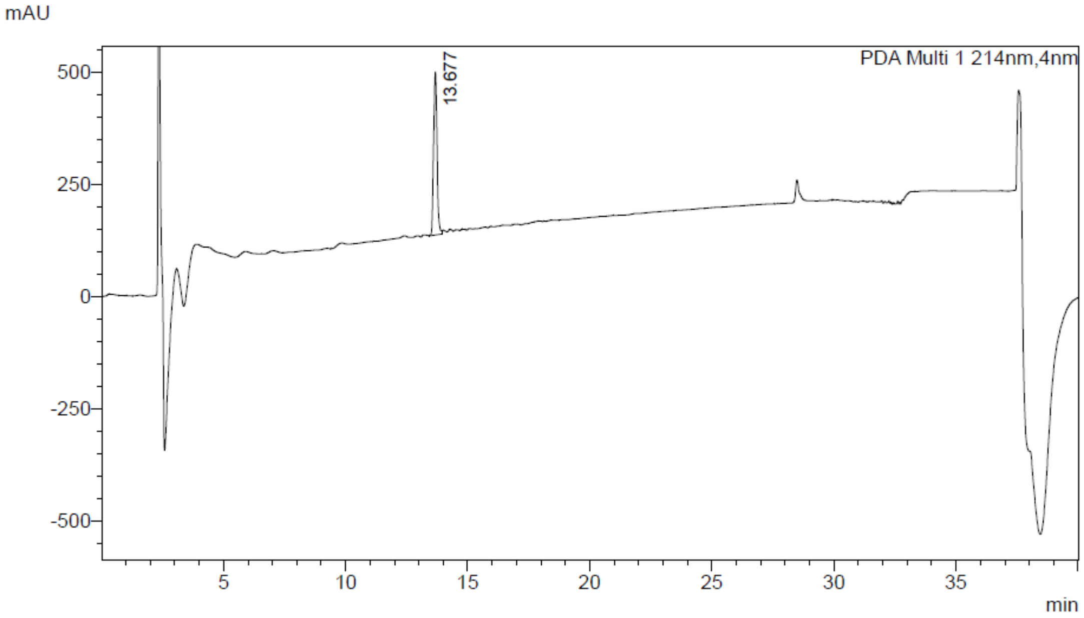

Supplementary Figure 37 Analytical HPLC result for FAM-DAPK1.